Design, Synthesis, and Biological Activity of Pyridopyrimidine Scaffolds as Novel PI3K/mTOR Dual Inhibitors

Thibault Saurat,[†,‡] Frédéric Buron,[†] Nuno Rodrigues,[†] Marie-Ludivine de Tauzia,[‡] Lionel Colliandre,[†] Stéphane Bourg,[†,‡] Pascal Bonnet,[†] Gérald Guillaumet,[†] Mohamed Akssira,[§] Anne Corlu,[∥] Christiane Guillouzo,[∥] Pauline Berthier,[⊥] Pascale Rio,[⊥] Marie-Lise Jourdan,[⊥] Hélène Bénédetti,[‡] and Sylvain Routier*,[†]

[†]Institut de Chimie Organique et Analytique, Université d'Orléans, UMR CNRS 7311, Rue de Chartres, BP 6759, 45067 OrléansCedex 2, France

[‡]Centre de Biophysique Moléculaire, CNRS Orléans, Rue Charles Sadron, 45071 Orléans, France

[§]Équipe de Chimie Bioorganique & Analytique, URAC 22, Université Hassan II Mohammedia-Casablanca, BP 146, 28800 Mohammedia, Morocco

[∥]Hôpital de Pontchaillou, Université de Rennes 1, INSERM, UMR-991, 65033 Rennes Cedex, France

[⊥]Faculté de Médecine, Centre Hospitalier Universitaire (CHU) Tours, INSERM U1069, 10 Boulevard Tonnellé, 37032 Tours Cedex, France

S Supporting Information

ABSTRACT: The design, synthesis, and screening of dual PI3K/mTOR inhibitors that gave nanomolar enzymatic and cellular activities on both targets with an acceptable kinase selectivity profile are described. A docking study was performed to understand the binding mode of the compounds and to explain the differences in biological activity. In addition, cellular effects of the best dual inhibitors were determined on six cancer cell lines and compared to those on a healthy diploid cell line for cellular cytotoxicity. Two compounds are highly potent on cancer cells in the submicromolar range without any toxicity on healthy cells. A more detailed analysis of the cellular effect of these PI3K/mTOR dual inhibitors demonstrated that they induce G1-phase cell cycle arrest in breast cancer cells and trigger apoptosis. These compounds show an interesting kinase profile as dual PI3K/mTOR tool compounds or as a chemical series for further optimization to progress into in vivo experiments.
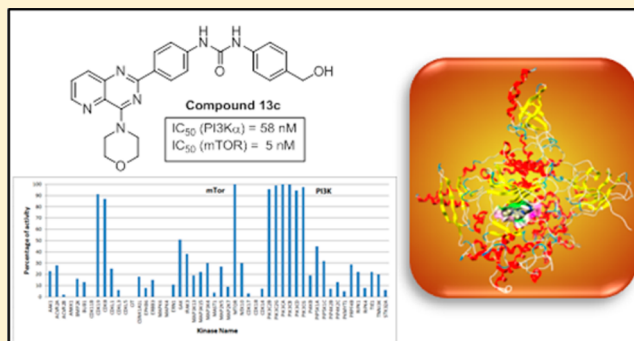
INTRODUCTION

The PI3K/Akt/mTOR pathway is associated with several receptor tyrosine kinases (RTKs) and G-protein-coupled receptors (GPCRs). PI3K (phosphoinositide 3-kinase), the first enzyme of the pathway, is a ubiquitous lipid kinase involved in a large variety of diseases. It catalyzes the transformation of phosphatidylinositol 4,5-diphosphate (PIP2) into phosphatidylinositol 3,4,5-triphosphate (PIP3).[1] Four PI3K isoforms[2] have been reported: PI3Kα in cancer,[3,4] PI3Kβ, which is more active in thrombosis-related phenomena,[5] and PI3Kδ in allergies and PI3Kγ in inflammatory responses.[6]

PI3Kα plays a significant role in cancer-related diseases and more specifically in insulin signaling.[7−10] In addition, cancers are also associated with mTOR (mammalian target of rapamycin), the third kinase of the signaling pathway studied in the present research work, whose main targets are S6K1,

which plays a key role in protein synthesis, and 4E-BP1, an actor in the translation initiation.[11]

In cancer, tumors exhibit a high frequency of activating mutations in the PI3K, Akt, and mTOR coding genes, leading to an elevated pathway activity and resulting in extended survival, growth, and angiogenesis of tumor cells.[12,13] Activation of the pathway is not vertical. It has been shown that mTOR exerts a negative feedback loop on PI3K: mTOR once activated will inhibit PI3K through IRS-1 (insulin receptor substrate 1).[14] Furthermore, it has been observed in several studies that external factors (growth factors, nutrient intake) can activate Akt and mTOR, thereby bypassing PI3K and thus restarting cancer genesis.[15,16]

For these reasons, the need to synthesize compounds that can inhibit the PI3K/Akt/mTOR pathway has been a great
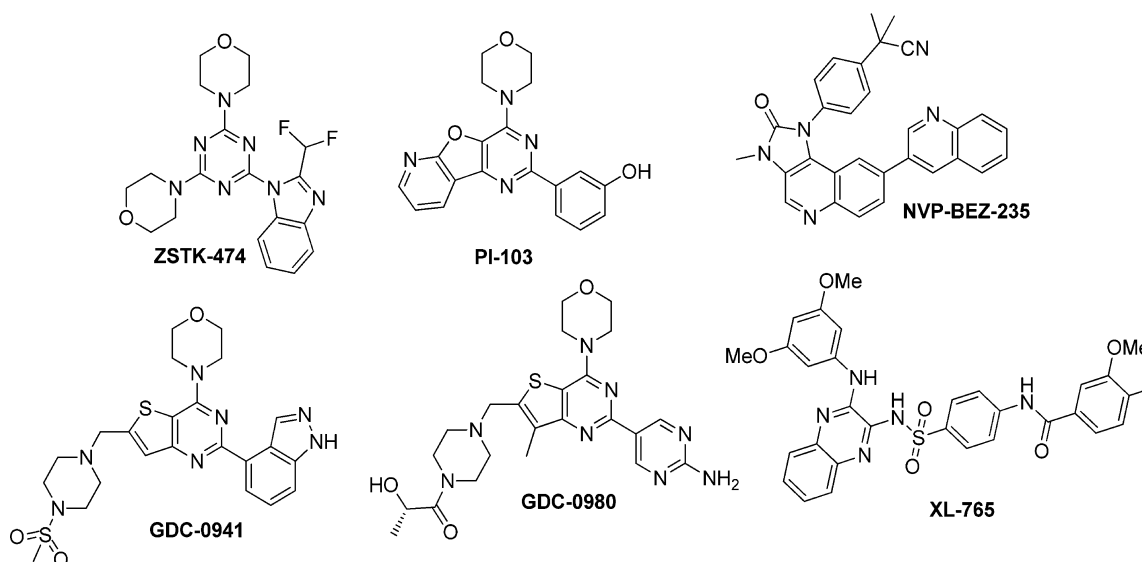
Figure 1. Examples of PI3K inhibitors.

motivation for research teams around the world.[17,18] In 2011, active drugs having an implication on PI3K, Akt, or mTOR were reported in more than 380 clinical trials. Three drugs have already been approved by the FDA (Food and Drug Administration) for mTOR (Afinitor, Torisel, and Zortress) but none yet for Akt or PI3K protein kinases. According to the National Cancer Institute, several drugs in phase I or II clinical trials are claimed as specific PI3Kα inhibitors.[19]

Most of these PI3Kα inhibitors share similar structural and chemical features, i.e., a central six-membered heterocycle substituted by a morpholine and a (hetero)aromatic cycle having a hydrogen bond donor group (Figure 1, ZSTK-414, GDC-0941, GDC-0980, PI103). As mentioned in the pathway functioning, due to the existence of a regulatory feedback loop, an independent activation of mTOR or PI3K alone is not sufficient to block the signaling pathway efficiently in cancer cells.[20] It is therefore crucial to consider the combined inhibition of both enzymes.[21] To our knowledge, only a few drugs that affect PI3Kα and mTOR together are in an early phase of clinical trials. NVP-BEZ-235, XL765, and an orally available candidate, GDC-0980, are claimed to be dual PI3K/mTOR inhibitors.[22]

We recently developed a straightforward methodology able to selectively functionalize 2,4-dichloropyridopyrimidine by two successive S_NAr and Suzuki cross-coupling reactions.[23] We thus envisioned applying our method to the design of a dual PI3Kα/mTOR inhibitor library. In this report, we report the synthesis of newly formed pyrido[2,3-d]- and pyrido[3,2-d]pyrimidine libraries **I** and **II** starting from a dichloro derivative of type **III** or **IV** (Figure 2).

After introducing an amine and a (het)aryl at C-2 or C-4, we established a complete SAR study using PI3Kα, PI3Kδ, PI3Kγ,

and mTOR as biological targets. In silico modeling studies were used to support medicinal chemistry efforts and proved to be successful in explaining the SAR of the tested compounds. Finally, the effects of the seven best inhibitors were measured on three cancer cell lines and normal fibroblasts. Further investigations were carried out for the two best compounds, which were tested on three other cancer cell lines and were shown to affect PI3K and mTOR activities in these cells, to block their cell cycle in the G1-phase, and to induce apoptosis.

RESULTS AND DISCUSSION

Synthesis and Kinase Assays. The derivatives **3a−g** were obtained after a two-step synthesis from 2,4-dichloropyrido-[3,2-d]pyrimidine (**1**). S_NAr regioselectively occurred at C-4 using aliphatic primary or secondary amines in the presence of Et_3N at room temperature and afforded compounds **2a−g** in satisfying yields (Scheme 1, Table 1). In the second step, the 3-

Scheme 1[a]
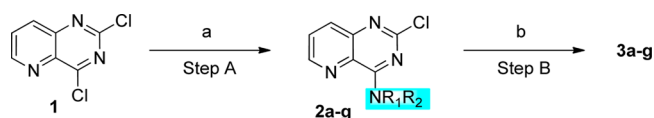
[a]Reagents and conditions: (a) amine, Et_3N, THF, rt, 12 h; (b) 3-$HOC_6H_4B(OH)_2$, K_2CO_3, $Pd(PPh_3)_4$, DME, MW, 150 °C, 1 h. For yields see Table 1.

hydroxyphenyl group was introduced using a Suzuki cross-coupling reaction under microwave irradiation to improve the yields, which are very low otherwise. This palladium-catalyzed reaction gave access to the attempted compounds in good to excellent yields, except in the case of **3f** (entry 6), which was only detected as molecular traces.

The six final products (**3a−e** and **3g**) were evaluated for their PI3K inhibition potency (Table 1). Morpholine seems essential to strongly diminish PI3Kα activity, and the IC_{50} was measured in the nanomolar range.[24] Replacement of this core by other cyclic amines causes a dramatic decrease in activity despite the presence of electron-rich atoms.
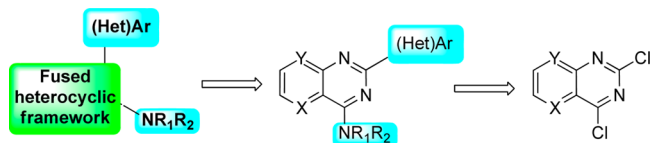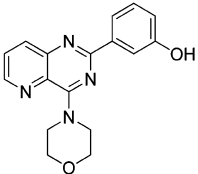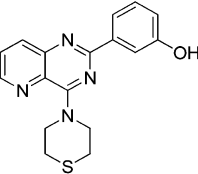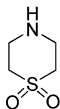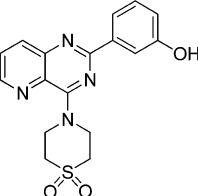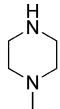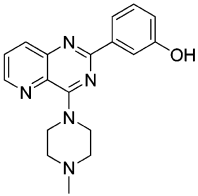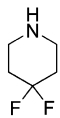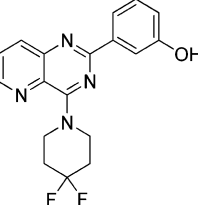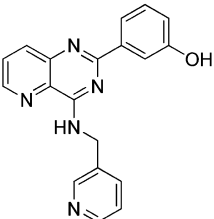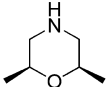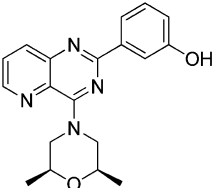

Figure 2. Disubstituted pyridopyrimidine libraries **I** and **II** from precursors **III** and **IV**.

Table 1. Synthesis Yields and Biological Evaluation of Compounds 3a–g

Entry	Step A R₁R₂NH	Compound	Yield[a]	Step B Compound		Yield[a]	IC₅₀ against PI3K kinases (μM)[b] PI3Kα	PI3Kγ	PI3Kδ
1	(morpholine)	2a	89%	(structure)	3a[24]	76%	0.019	0.031	0.003
2	(thiomorpholine)	2b	75%	(structure)	3b	76%	31.8	>50	>50
3	(thiomorpholine dioxide)	2c	58%	(structure)	3c	85%	>50	>50	>50
4	(N-methylpiperazine)	2d	85%	(structure)	3d	87%	>50	>50	>50
5	(4,4-difluoropiperidine)	2e	80%	(structure)	3e	61%	>50	>50	>50
6	(pyridinylmethanamine)	2f	61%	(structure)	3f	traces	-	-	-
7	(2,6-dimethylmorpholine)	2g	87%	(structure)	3g	85%	1.4	0.574	0.687

[a]Yields are indicated for isolated products. [b]IC₅₀ values are presented as the mean of a triplicate experiment. Standard deviations are reported in Table S1 of the Supporting Information.

As oxygen seems to be essential for activity,[25] we used 2(R),6(R)-dimethylmorpholine to obtain **3g** (entry 7), but its activity dropped to the micromolar range. Finally, **3a** remains the best compound, showing comparable IC₅₀ values against PI3Kα and PI3Kγ and a remarkable potency for the δ isoform (IC₅₀ = 3 nM).
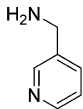
Thus, we conserved the morpholino group to pursue our investigation and further explore the SAR. For the next C-2 (het)Ar optimization (Scheme 2), we successfully achieved the cross-coupling reactions using several commercially available arylboronic acids or potassium aryltrifluoroborates (1.5 equiv) under the conditions described above.

Scheme 2[a]
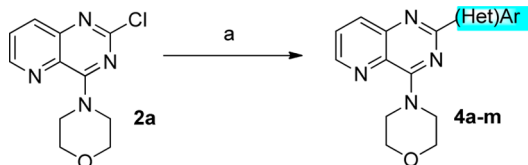
[a]Reagents and conditions: (a) (Het)ArB(OH)$_2$ or (Het)ArBF$_3$K, K$_2$CO$_3$, Pd(PPh$_3$)$_4$, DME, MW, 150 °C, 1 h. For yields see Table 2.

The desired products **4a−m** were isolated in moderate to excellent yields (Table 2). Variations in the efficiency of the cross-coupling reaction were mostly related to the purification step. Most of the reaction appeared to be complete during the monitoring. Derivatives **4g** and **4h** (entries 8 and 9) were easily obtained from a cross-coupling reaction between **2a** and the corresponding nitrophenylboronic acid, followed by reduction of the nitro group using stannous chloride. In a complementary single-step synthesis, we also prepared the mono- and bisacetylated derivatives **5** and **6** from **4m** in the same reaction using an excess of Ac$_2$O in DMF under microwave irradiation in 28% and 44% yields, respectively (entries 15 and 16).

In vitro activities toward PI3K kinase isoforms were measured using the final compounds **4a−m**, **5**, and **6**, and

Table 2. Synthesis and Biological Evaluation of Derivatives 4

| Entry | Compound | Yield[a] | IC$_{50}$ (μM)[b] | | | Entry | Compound | Yield[a] | IC$_{50}$ (μM)[b] | | |
			PI3Kα	PI3Kγ	PI3Kδ				PI3Kα	PI3Kγ	PI3Kδ
1	**3a**	76%[c]	0.019	0.031	0.003	9	**4h**	70%[c,e]	>50	>50	11.13
2	**4a**	87%[c]	18.60	9.36	24.03	10	**4i**	76%[c]	11.92	>50	>50
3	**4b**	74%[c]	1.54	6.39	1.53	11	**4j**	45%[d]	1.36	7.88	26.50
4	**4c**	85%[c]	>50	>50	>50	12	**4k**[26]	49%[d]	0.555	3.40	5.28
5	**4d**	76%[c]	29.40	>50	>50	13	**4l**	23%[d]	0.027	0.087	0.008
6	**4e**[26]	88%[c]	0.061	0.183	0.024	14	**4m**[27]	72%[d]	0.007	0.081	0.029
7	**4f**	71%[c]	6.97	30.70	1.14	15	**5**	28%[f]	1.40	12.30	1.90
8	**4g**	57%[c,e]	2.50	6.30	0.150	16	**6**	44%[f]	>50	>50	>50

[a]Yields are given for the isolated product. [b]IC$_{50}$ values are presented as the mean of a triplicate experiment. Standard deviations are reported in Table S1 of the Supporting Information. [c]Boronic acid was used. [d]Potassium trifluoroborate was used. [e]Overall yield of two steps. [f]Compounds **5** (28%) and **6** (44%) were obtained from **4m** using Ac$_2$O (10.0 equiv) and DMF (120 °C, 30 min).

the IC_{50} values were compared to that of **3a** (entry 1). The best position for the OH phenol group remains at the *meta* position since its position shift to *ortho* or *para* leads to an overall inactivation of the drugs. The hydrophilic character and the ability of the drug to create a hydrogen bond in this region are certainly crucial as proposed from docking results. Spacing the OH group by addition of a methylene kneecap in the *meta* position of the phenyl ring was well tolerated (**4e** vs **4f**, entries 6 and 7), whereas methyl ethers **4c** and **4d** were also totally inactive (entries 4 and 5).

Replacement of the phenyl hydroxyl group by a primary amine or the phenol by a 3-pyridine or a 4-indazole (entries 8–11) led to poorly active compounds **4i** and **4j**.[28] Nevertheless, with the 4-indazole-containing derivative **4k**, we observed a global increase of activity for PI3Ks and in particular for the α isoform (entry 12).

It appears that 2-aminopyridine and -pyrimidine moieties could be used as phenol isosters (entries 13 and 14). PI3Kα and PI3Kδ were more affected by the two novel lead compounds. **4m**, which inhibits PI3Kα with a remarkable IC_{50} of 7 nM, is the most selective inhibitor ever designed in the disubstituted pyridopyrimidine series. The activity of the 2-aminopyrimidine-containing compound is due to the presence of an acidic hydrogen atom since acetylated compound **5** remains slightly active and diacetylated **6** is fully inactive (entries 15 and 16).[29]

To pursue the SAR exploration, we next investigated successively the effect of reversing the C-4 morpholine and the C-2 phenol groups on the pyrido[3,2-*d*]pyrimidine scaffold and of the switch of the central core for the [2,3-*d*] regioisomer (Scheme 3, Table 3).[30] To obtain the expected derivatives, we adapted the previously reported robust synthetic methods and used the dichloro derivatives **1** and **10** as starting materials.

For the synthesis of the "inverso" derivative **9**, 3-(methoxymethoxy)phenyltrifluoroborate potassium was prepared to perform the Suzuki cross-coupling reaction.[31] The palladium-catalyzed reaction occurred selectively using a near stoichiometric amount of boronic acid in refluxing toluene at 100 °C for 2 h with our classical catalytic system and yielded **7**

in 45% yield. The C-2 S_NAr was next carried out with morpholine and Et_3N in refluxing THF and gave the desired compound **8** in 68% yield. Finally, the MOM protective group was removed with HCl (4 N in dioxane) at room temperature to afford **9** in 60% yield.

For the compound synthesis in the pyrido[2,3-*d*]pyrimidine series, compound **10** was subjected to the reactions leading to compounds **2** and **3** from **1**. Derivatives of type **12** were isolated in fair yields.

The derivative **9** showed an inhibition of PI3Kα (IC_{50} = 59 nM) which was still 3-fold less efficient than that of **3a**, whereas against the γ and δ isoforms, dramatic decreases in activity were observed (IC_{50}(PI3Kγ) = 1.06 μM, IC_{50}(PI3Kδ) = 0.186 μM). The same general behavior was observed with pyrido[2,3-*d*]pyrimidine compounds **12a−c**; activities were partially lost especially for the PI3Kα and PI3Kγ isoforms (vs the corresponding compound **3a** in the [3,2-*d*] series, Table 3). Noteworthy, the preservation of the activity of compound **12c** against PI3Kδ is observed, leading to incipient selectivity against other isoforms.

The last modification we performed is entirely based on the mTOR inhibitor discovery which mainly uses a urea to enhance binding.[32] Consequently, we prepared and evaluated ureas of type **13**. For this new proposal, the anilines **4g** and **4h** were converted to the corresponding in situ formed isocyanates by treatment with triphosgene in the presence of an excess of DIPEA in THF at −78 °C, and the unstable intermediates were immediately trapped with various amines to afford products **13** with moderate to good yields (Scheme 4 and Table 4).

Regarding both the biological activity on PI3Kα and the nature of the urea substituents, a small methyl is well tolerated (entry 1), up to the size of a six-membered ring. To maintain the kinase inhibition, urea is better positioned in the *para* position of aryl ring A (Table 4, entry 3 vs entry 8), indicating some additional interactions in the ATP binding pocket. In addition, if R bears a supplementary donor or acceptor of hydrogen bonds, the global activity increases.

For this novel function, a hydroxymethyl is preferred in the *meta* position, whereas a simple hydroxyl is better tolerated in the *para* position (entry 2 vs entry 3 and entry 5 vs entry 4). In the pyridine series (entries 6 and 7), the *m*-nitrogen atom interacts better with the biological targets. Except for **13c** and **13h**, the urea derivatives are more active on PI3Kα and PI3Kγ than on the PI3Kδ isoform. The most selective compound is indubitably **13e** (entry 5), which exhibits a selective action on the α isoform (5- and 10-fold more potent compared to the γ and δ isoforms, respectively).

Since mTOR and PI3K conserved a typical ATP site despite their little kinase fold resemblance, we focused on the inhibitory effect of our compounds on mTOR. As it turns out, all of our compounds displayed submicromolar activities against both mTOR and PI3Kα (Table 5). Our dual inhibitors are more efficient at inhibiting PI3Kα than mTOR (entries 1−8). However, our best PI3Kα inhibitors, **3a** and **4n**, displayed very good nanomolar inhibitions against mTOR (entries 1 and 4).
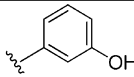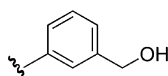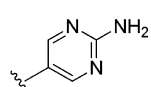
Other derivatives such as **12a**, **12b**, **13e**, and **13f** have similar activity ratios on the two kinases (entries 6, 7, 13, and 14). Interestingly, the introduction of an aryl urea on ring B led to compounds which are more active against mTOR than against PI3Kα (entries 9−12). Compounds **13b** and **13c** in particular displayed the strongest activities (IC_{50} = 1 and 5 nM,

Scheme 3[a]
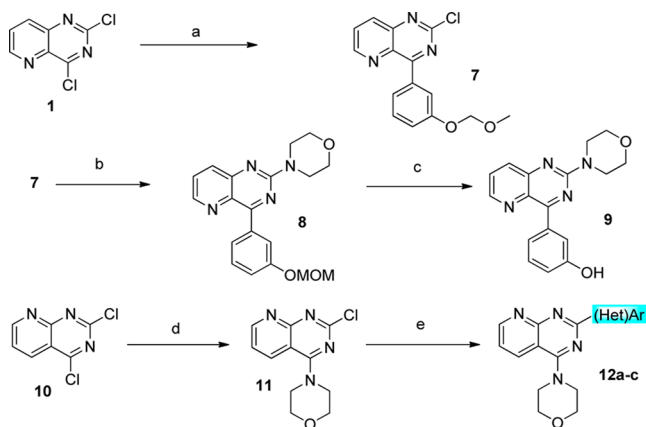
[a]Reagents and conditions: (a) 3-(MOM)$C_6H_4BF_3K$, K_2CO_3, Pd-(PPh$_3$)$_4$, toluene, 100 °C, 2 h, 45%; (b) morpholine, Et$_3$N, THF, reflux, 12 h, 68%; (c) HCl (4 N), EtOH, rt, 1 h, 60%; (d) morpholine, Et$_3$N, THF, rt, 12 h, 80%; (e) (Het)ArB(OH)$_2$ or (Het)ArBF$_3$K, K_2CO_3, Pd(PPh$_3$)$_4$, DME, MW, 150 °C, 1 h. For exact structures and yields see Table 3.

Table 3. Synthesis and Biological Evaluation of Pyrido[2,3-d]pyrimidine-Type Compounds

Entry	(Het)Ar	Compounds (Yield)[a]	IC$_{50}$ (μM)[b]		
			PI3Kα	PI3Kγ	PI3Kδ
1		**12a** (60%)	0.106	0.741	0.367
2		**12b** (65%)	0.268	>50	7.60
3		**12c** (69%)	0.144	4.70	0.018

[a]Yields are indicated for isolated products. [b]IC$_{50}$ values are presented as the mean of a triplicate experiment. Standard deviations are reported in Table S1 of the Supporting Information.

Scheme 4[a]

[a]Reagents and conditions: (a) triphosgene, DIPEA, THF, −78 °C, 40 min, then RNH$_2$, DIPEA, THF, rt, 24 h. For exact structures and yields see Table 4.

respectively) on mTOR, the last kinase in the pathway (entries 10 and 11).

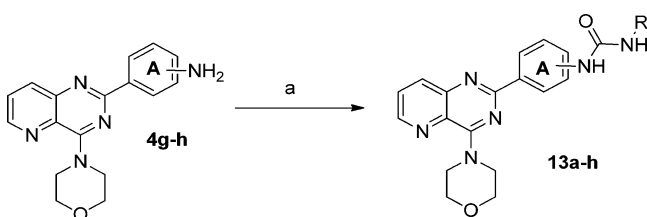Finally, we examined the selectivity profile of **13c** on a diverse 50-kinase panel. The activity of the compound was confirmed on the PI3K family and mTOR, and the compound appeared to be very selective toward other kinases with the exception of CDK19 and CDK8 (Table 6).

Molecular Modeling. Docking studies were carried out to investigate the binding mode of our compounds in the PI3Kα isoform. Among numerous crystallographic structures of PI3K, only three were available for the α isoform of human PI3K. Two apo structures (PDB entries 2RD0 and 3HIZ)[33−35] and one complex with the covalent inhibitor wortmannin (PDB entry 3HHM)[33] were used as structural models of PI3Kα in our studies. Among all the crystallographic structures of PI3K, a majority contain reversible inhibitors that provide useful information on protein/ligand interactions found in their active site. More importantly, some of these inhibitors are structurally similar to our compounds. The strong sequence and structural similarities between the different classes and isoforms of PI3K (especially in their active sites)[36] suggest that the interactions observed with these crystallographic inhibitors are likely to occur for our compounds.

To select the best model for docking experiments, wortmannin and seven PI3Kγ cocrystallized inhibitors (ligands containing a pyrimidine 2-morpholino-4-heteroaryl or substituted 2-heteroaryl-4-morpholine motif) were docked in the three previously selected structures. The use of the 3HHM structure enabled the reproduction of the crystallographic binding modes of the ligands. Nevertheless, the hydrogen bond interaction seen in the original complex between the ligand and the side chain of the catalytic Lys802 was not reproduced for two thienopyrimidine derivatives (PDB entries 3L16 and 3L17)[29] and a pyrazolopyrimidine derivative (PDB entry 3IBE).[39]
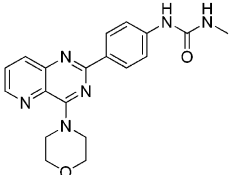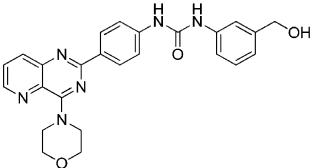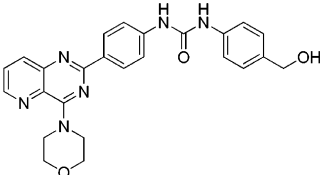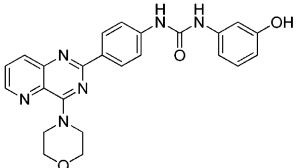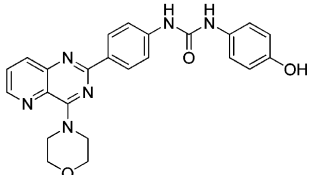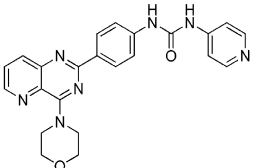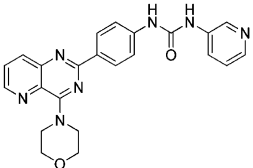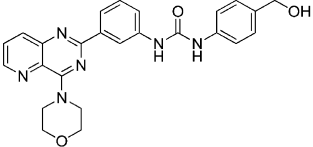
After careful analysis of the active site, we established that these ligands need a different conformation of the flexible lateral chain of the catalytic Lys802 to correctly bind to our docking model. The conformation of the corresponding lysine observed in the structure of PI3Kγ in complex with the pyrazolopyrimidine derivative (PDB entry 3IBE) was manually assigned to Lys802 in the 3HHM structure. The use of this new model enabled all interactions to be reproduced for each docked inhibitor in the corresponding original structures. It was thus used for all further docking experiments.

Next, our ligands were docked using the previously validated model. The 10 best docking poses according to GlideScore[38] were conserved for each ligand. All the compounds adopted orientations analogous to those of the cocrystallized inhibitors. The binding is driven by one hydrogen bond created between the oxygen atom of the morpholino group and the NH group of Val851 in the hinge region of the active site (Figure 3). This hydrogen bond is considered as the key interaction that confers the binding capacity on the ligands. The strength of this hydrogen bond (or its absence) explains why the activity of our compounds decreases (or disappears) when the oxygen atom of the morpholino group is modified (**3a** ≫ **3b** ≫ **3c**).

The binding of the morpholino group to the hinge region leads to the orientation of the aryl group toward Asp810 and the catalytic Lys802. The hydroxyl position on this aryl group has a drastic influence on the activity of the compounds (Table 4). Docking of **3a** shows that the hydroxyl function replaces a conserved water molecule, as has already been shown in some crystallographic structures of sufficient resolution (PDB entries 3L54, 3L08, and 3ML9).[22b] This hydroxyl function forms two hydrogen bonds with the oxygen atom of the hydroxyl group of Tyr836 and with one oxygen atom of the carboxyl group of Asp810 (Figure 3). Moreover, the hydroxyl function of compound **4e** forms the same hydrogen bonds, slightly moving the pyrido[3,2-d]pyrimidine moiety in the active site.
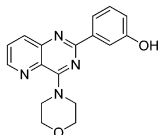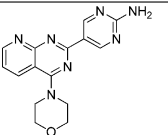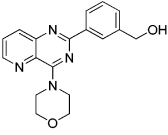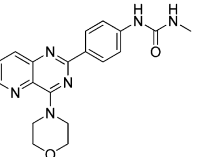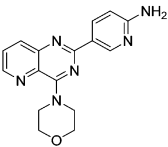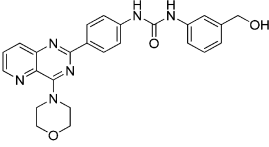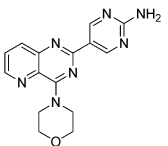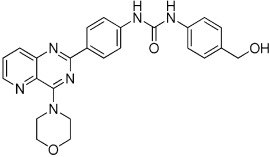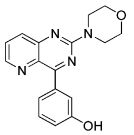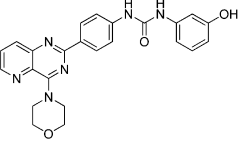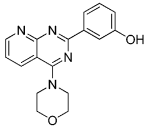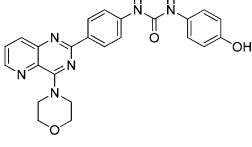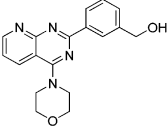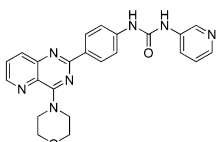
The docking of the pyrido[2,3-d]pyrimidine isomer derivatives (compounds **12a−c**) does not show significant differences in the global binding mode compared to that of the previous scaffold. Only a minor influence can be observed on the conformation of the morpholino group due to the introduction

Table 4. Synthesis Yields and Biological Evaluation of Ureas 13

Entry	Compound		Yield[a]	IC$_{50}$ (μM)[b]		
				PI3Kα	PI3Kγ	PI3Kδ
1		**13a**	21%	0.092	0.227	0.077
2		**13b**	40%	0.040	0.062	0.104
3		**13c**	89%	0.058	0.026	0.014
4		**13d**	45%	0.171	0.353	0.770
5		**13e**	58%	0.045	0.264	0.449
6		**13f**	71%	0.317	0.153	0.565
7		**13g**	69%	0.045	0.079	0.134
8		**13h**	47%	5.8	22	0.836

[a]Yields are given for isolated products. [b]IC$_{50}$ values are presented as the mean of a triplicate experiment. Standard deviations are reported in Table S1 of the Supporting Information.

Table 5. IC$_{50}$ Values of the Best Inhibitors against PI3Kα and mTOR

Entry	Compound		IC$_{50}$ (μM)[a]		Entry	Compound		IC$_{50}$ (μM)[a]	
			PI3Kα	mTOR				PI3Kα	mTOR
1		3a	0.019	0.037	8		12c	0.144	0.400
2		4e	0.061	0.336	9		13a	0.092	0.013
3		4l	0.027	0.266	10		13b	0.040	0.001
4		4m	0.007	0.059	11		13c	0.058	0.005
5		9	0.059	0.453	12		13d	0.171	0.036
6		12a	0.106	0.100	13		13e	0.045	0.054
7		12b	0.268	0.127	14		13g	0.045	0.035

[a]IC$_{50}$ values are presented as the mean of a triplicate experiment. Standard deviations are reported in Table S1 of the Supporting Information.

of a hydrogen atom in position 5 of the scaffold. This could explain the lower activity of such compounds.

Inversion of the morpholino and aryl groups (compound **8**) does not induce any changes in the observed interactions of these groups but leads to a different orientation of the scaffold in the active site. The morpholino group still forms one hydrogen bond with Val851 in the hinge region, and the aryl group is still oriented toward Asp810 and the catalytic residue Lys802. The different orientation of the scaffold in the active site can explain the lower activity of this compound.

Using urea derivatives, the binding site of PI3Kα was explored beyond the catalytic Lys802 (compounds **13a−h**).

The predicted binding modes of the 4-urea derivatives are similar to that of the cocrystallized substituted pyrazolopyrimidine inhibitor (PDB entry 3IBE), with the morpholino group still forming one hydrogen bond with Val851 in the hinge region. Nevertheless, some differences can be noticed. The crystallographic complex shows that the urea function forms three hydrogen bonds with the target. Each NH group of the urea forms a hydrogen bond with the oxygen atom of the carbonyl group of the side chain of Asp810, whereas the carbonyl group of the urea forms one hydrogen bond with the side chain of Lys802. In our docking poses, four hydrogen bonds can be observed. Due to a slightly different orientation of

Table 6. Protein Kinase Selectivity of 13c in a Kinase Interaction Assay (KinomeScan)[a]

kinase	ctrl (%)	kinase	ctrl (%)	kinase	ctrl (%)	kinase	ctrl (%)	kinase	ctrl (%)
AAK1	77	CDKL3	94	IRAK3	62	PCTK3	100	PIP5K1C	68
ACVR2A	72	CDKL5	100	LZK	81	PFTK1	93	PIP5K2B	93
ACVR2B	98	CIT	100	MAP3K15	78	PIK3C2B	4.2	PIP5K2C	87
ANKK1	100	CSNK1A1L	82	MAP3K4	70	PIK3C2G	0.95	PKMYT1	95
BIKE	84	EPHB6	92	MAST1	96	PIK3CA	0	PRP4	71
BUB1	87	ERBB3	85	MEK5	73	PIK3CB	0.15	RIPK1	78
CDC2L1	100	ERK3	100	MKK7	91	PIK3CD	5.4	RIPK4	92
CDK11	8.8	ERK4	100	MTOR	0	PIK3CG	2.5	TIE1	78
CDK8	13	ERN1	89	NEK10	70	PIK4CB	81	TNNI3K	80
CDKL1	75	GAK	49	PCTK2	97	PIP5K1A	55	YANK1	94

[a]13c was screened at a 10 μM concentration on a 50-kinase interaction panel, and results for primary screen binding interactions are reported as "ctrl (%)", where lower numbers indicate stronger hits.
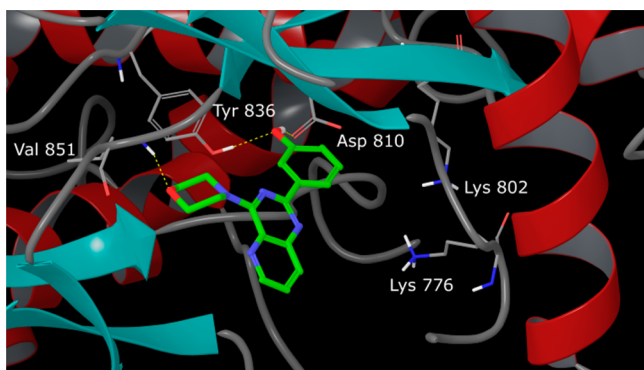
Figure 3. Representation of the predicted binding mode of compound **3a** in the active site of PI3Kα. Hydrogen bonds are represented in yellow-black dotted lines. For clarity, only polar hydrogens are represented and residues 767−772 overlaying the ligands are hidden in the ribbon representation (PDB reference codes 3HHM and 3IBE for the positioning of Lys802).

the side chain of Asp810 in our model, the NH groups of the urea of the docked ligands form two hydrogen bonds with the same oxygen atom of the carbonyl group of the side chain of Asp810. Moreover, the carbonyl group of the urea forms one hydrogen bond with the amino groups of the side chains of Lys802 (Figure 4). Lys776 is highlighted too because some poses of our different docked compounds form a hydrogen
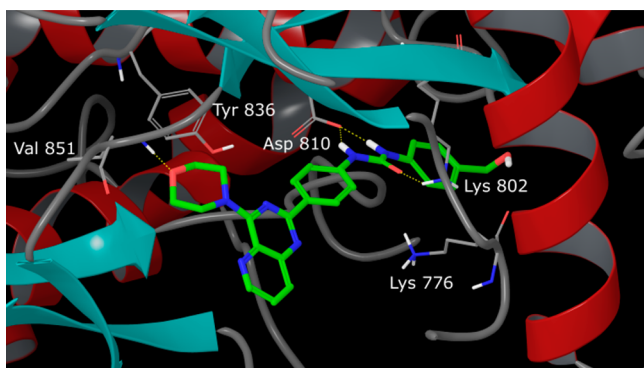
Figure 4. Representation of the predicted binding mode of compound **13c** in the active site of PI3Kα. Hydrogen bonds are represented in yellow-black dotted lines. For clarity, nonpolar H atoms are not represented and residues 767−772 overlaying the ligands are hidden in the ribbon representation (PDB reference codes 3HHM and 3IBE for the positioning of Lys802).

bond with this lysine (not shown), instead of the neighboring Lys802. This interaction is not present in the crystallographic structure because the conformation of the lysine in PI3Kγ (PDB entry 3IBE) corresponding to Lys776 could not be defined, probably due to its flexibility.

This study shows that our ligands adopt binding modes in PI3Kα that are similar to those of known inhibitors in PI3Kγ. Crystallographic studies of the complexes between PI3Kα and our ligands should be considered to confirm the predicted binding modes. In particular, these studies would enable the identification of important residues in the PI3Kα active site forming key interactions with the inhibitors (Lys776, Lys802, Asp810). This information would lead to a better optimization of our compounds.

Cellular Assays. Compounds which exhibited dual activity on PI3Kα and mTOR with IC$_{50}$ values lower than 100 nM were selected for a primary cellular screening assay using six cancer cell lines (Tables 7 and 8): hepatocellular colorectal and mammary carcinoma cells and immortalized keratinocytes. Human diploid skin fibroblasts were used as noncancer cells.

Table 7. Cancer Cell Lines and Their PI3K Signaling Pathway Status

cell line	human cell type	mutation	pathway overactivation	ref
Huh-7	hepatocellular carcinoma		yes	39−41
Caco-2	colorectal adenocarcinoma			42, 43
HaCaT	immortalized keratinocyte		elevated Akt activity	44−46
MCF-7	breast adenocarcinoma	PI3KCA	activated	47
MDA-MB-231			normal	47
MDA-MB-468		PTEN	over	47

First and foremost, our newly tested 2,4-disubstituted pyridopyrimidine did not affect the survival and proliferation of human skin fibroblasts. Regarding cancer and immortalized cell lines, the most potent PI3Kα inhibitors **3a** and **4m** (Table 5, entries 1 and 4) act in the same concentration range as PI103 but do not appear to be the best products with respect to cell toxicity. The results clearly show that the best in cellulo inhibitory effects were obtained with the best dual PI3K and mTOR inhibitors and more particularly with the more potent mTOR inhibitors **13b** and **13c**.

Table 8. In Cellulo Activity of the Best Inhibitors, IC$_{50}$ (μM)^a

entry	compd	Huh-7 (liver)	Caco-2 (colon)	HaCaT (skin)	no. of fibroblasts	breast^c		
						MCF-7	MDA-MB-231	MDA-MB-468
1	**3a**	2	3	3	>25			
2	**4m**	3	3	4	>25			
3	**13a**	5	2.5	3	>25			
4	**13b**	0.5	1	1	>25	0.25	0.5	0.8
5	**13c**	0.5	0.6	0.5	>25	0.2	0.25	0.1
6	**13e**	2	2	1	>25			
7	**13f**	2	2	2	>25			
8	**PI103**^{b}	5	2	2	>25			

^{a}IC$_{50}$ values are presented as the mean of a triplicate experiment. ^{b}We used PI103 as the reference compound.[37] ^{c}Only **13b** and **13c** were tested on three breast cancer cell lines.
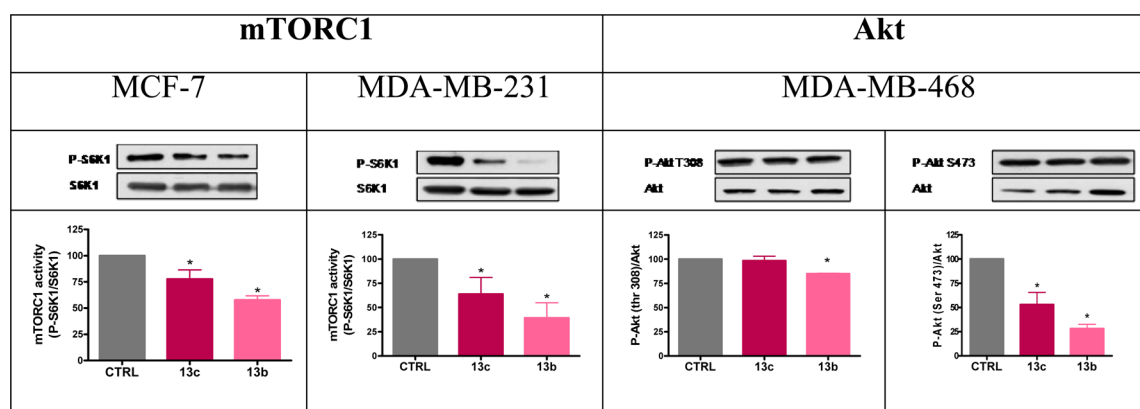
Figure 5. Effects of **13b** and **13c** on the AKT and mTORC1 activity in breast cancer cells by Western blotting.
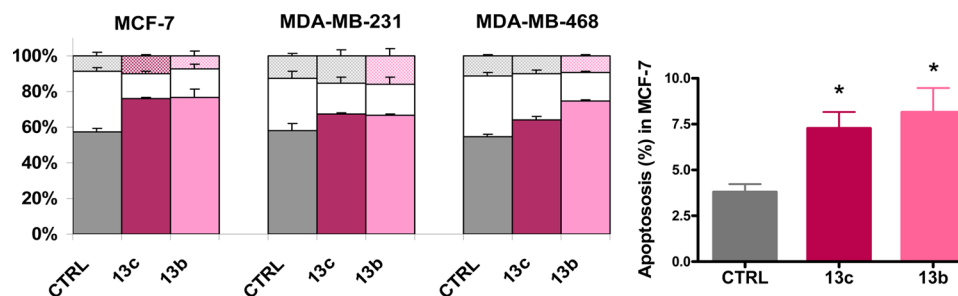
Figure 6. Effects of the best inhibitors **13b** and **13c** on the growth of breast cancer cell lines: left, distribution in the cell cycle; right, rate of apoptosis.

The best cellular effects were measured with the dual inhibitors **13b** and **13c** showing IC$_{50}$ values around 50 nM on PI3K and close to nanomolar IC$_{50}$ values on mTOR (Table 8, entries 4 and 5). For these two compounds, the micromolar barrier is reached. For **13a**, **13e**, and **13f**, the partial decrease of PI3K or mTOR inhibition as compared to **13b** and **13c** resulted in a cell survival enhancement.

Since the PI3K pathway is frequently activated in human breast cancers and activation is associated with a poor prognosis and resistance to treatment,[48] the most cytotoxic derivatives **13b** and **13c** were further tested on three additional breast cancer cell lines differing in their level of PI3K pathway activation (Table 7). A high activity of the best inhibitors **13b** and **13c** was observed on all cell lines, as can be seen by the IC$_{50}$ values. The IC$_{50}$ values of **13c** were 200 and 250 nM for MCF-7 and MDA-MB-231, respectively. The best inhibition (IC$_{50}$ = 100 nM) was obtained with **13c** on MDA-MB-468, the cell line harboring a PTEN mutation and thus an overactivation of the PI3K pathway.

To ensure that **13b** and **13c** do inhibit PI3Kα and mTOR inside the cells, we checked by Western blotting the activity of the two major kinases of the pathway, Akt and mTORC1 (one of the two protein complexes containing mTOR), after treatment with inhibitors at the IC$_{50}$ level (Figure 5).

mTORC1 activity was evaluated by quantifying the phosphorylation level of its target, S6K1, in the MCF-7 and MDA-MB-231 cell lines. mTORC1 was well inhibited in the two cell lines with both inhibitors; the best reduction was observed with **13b**, which is the most active compound against mTOR.

Akt activity was monitored by measuring its phosphorylation level on Thr308 and Ser473 in MDA-MB-468, the cell line expressing high levels of activated Akt. Both inhibitors reduced p-AKT Ser473 (the mTORC2 target, the other protein complex containing mTOR), while P-Akt Thr308 (the PDK1 target, a downstream kinase, in the PI3K pathway) was slightly reduced by **13b** only. These results are in accordance with the results of enzymatic assays which show a more potent efficiency

for **13b** as compared to **13c** to inhibit PI3Kα and mTOR. A discrepancy was observed with proliferation assay results since **13c** appeared to be the most efficient to reduce cell proliferation. This could be explained by the poor sensitivity of the MTT (3-(4,5-dimethylthiazol-2-yl)-2,5-diphenyltetrazolium bromide) assay.

As cytotoxicity may result from inhibition of proliferation and/or an increase in apoptosis, we studied the effects of **13b** and **13c** on the distribution in the cell cycle and on apoptosis of the three breast cancer cell lines by flow cytometry.

The G2/M-phase was not affected. In MCF-7 and MDA-MB-468 cells, the S-phase was reduced while the G1-phase was increased compared to the controls, implying that both inhibitors blocked the cell cycle at the G1-phase (Figure 6). Although the treatments changed the distribution of MDA-MB-231 cells in the same way as they did for MCF-7 and MDA-MB-468 cells, the changes were not statistically significant. This differential effect on the cell lines may be related to the level of PI3K pathway activation. Inhibitors are more efficient in cells harboring high levels of their target. Apoptosis was induced in MCF-7 by **13b** and **13c** inhibitors as seen in Figure 6. It was also increased in MDA-MB-231 and MDA-MB-468 but not significantly (data not shown).

In summary, the ureas **13b** and **13c** are the best candidates to reduce proliferation of all the cancer cell lines tested. In breast cancer cells, the inhibition of their targets PI3Kα and mTOR is associated with an arrest of cells in the G1-phase along with an induction of apoptosis.

■ CONCLUSION

A new class of 2,4-disubsituted pyrido[3,2-*d*]pyrimidines and 2,4-disubstituted pyrido[2,3-*d*]pyrimidines were prepared following a two-step synthesis involving an S$_N$Ar and a Suzuki-type cross-coupling reaction from our original 2,4-dichloropyridopyrimidine precursor. Biological activities were measured for each novel compound on three PI3K isoforms. The best candidates were additionally evaluated on mTOR to identify their potential activity as dual PI3K/mTOR inhibitors. The new library reported in this paper led to the discovery of seven promising dual PI3Kα/mTOR inhibitors which exhibited in vitro IC$_{50}$ values of less than 100 nM on both kinases. Structure−activity relationships are fully depicted, and molecular modeling studies explain the interaction of active compounds in the PI3Kα ATP binding site. In cellulo studies demonstrated that in vitro PI3K and mTOR inhibitions are related to cancer cell survival; a strong cytotoxic effect was observed. Indeed, the two urea derivatives which are the best dual PI3K and mTOR inhibitors specifically affect the survival and proliferation of cancer cell lines below the micromolar level. Further tests of the two lead compounds on breast cancer cell lines demonstrated that they do act on their two targets (PI3K and mTOR) inside the cells and reduce their proliferation by blocking them in the G1-phase of their cell cycle and by inducing apoptosis. Having in hand two lead compounds which fully appear as pro-apoptotic drugs, further efforts are in progress to enhance their therapeutic efficacy as anticancer agents. A particular focus will be made on bioavailability evaluation and ADME-tox studies.

■ EXPERIMENTAL PART

General Information. ^{1}H NMR and ^{13}C NMR spectra were recorded on a Bruker DPX 250 or 400 MHz instrument using CDCl$_3$ or DMSO-d_6. The chemical shifts are reported in parts per million (δ

scale), and all coupling constant (J) values are in hertz. The following abbreviations were used to explain the multiplicities: s (singlet), d (doublet), t (triplet), q (quartet), m (multiplet), and dd (doublet of doublets). Melting points are uncorrected. IR absorption spectra were obtained on a Perkin-Elmer PARAGON 1000 PC, and the values are reported in inverse centimeters. HRMS spectra were recorded on a Bruker maXis mass spectrometer. Monitoring of the reactions was performed using silica gel TLC plates (silica Merck 60 F$_{254}$). Spots were visualized by UV light at 254 and 356 nm. Column chromatography was performed using silica gel 60 (0.063−0.200 mm, Merck). Microwave irradiation was carried out in sealed 2−5 mL vessels placed in a Biotage Initiator system using a standard absorbance level (300 W maximum power). The temperatures were measured externally by an IR probe that determined the temperature on the surface of the vial and could be read directly from the instrument screen. The reaction time was measured from when the reaction mixture reached the stated temperature for temperature-controlled experiments. Pressure was measured by a noninvasive sensor integrated into the cavity lid.

The chromatographic purities of the final compounds were determined using an Agilent Technology 1260 Infinity HPLC system using a C18 column (Agilent ZORBAX Eclipse Plus, 3.5 μm, 4.6 mm × 100 mm) operating at 30 °C. Elution was carried out using acetonitrile containing 0.1% formic acid as mobile phase A and water containing 0.1% formic acid as mobile phase B. Elution conditions: at 0 min, 10% phase A + 90% phase B; at 5 min, 50% phase A + 50% phase B; at 7 min, 50% phase A + 50% phase B; at 7.1 min, 10% phase A + 90% phase B; at 20 min, 10% phase A + 90% phase B. The flow rate of the mobile phase was 0.9 mL/min, and the injection volume of the sample was 2 μL. Peaks were detected at 254 and 300 nm. The purities of all the tested compounds were found to be >95% unless otherwise stated.

General Procedure A for Amination at C-4 of the Pyridopyrimidine by S$_N$Ar. A solution of **1** or **10** (200 mg, 1.0 mmol, 1.0 equiv) in dry THF (20 mL) was cooled to 0 °C under an inert atmosphere. A solution of amine (1.05 equiv) and triethylamine (0.14 mL, 1.05 mmol, 1.05 equiv) in dry THF (5 mL) was added slowly. The mixture was stirred at room temperature for 12 h. The solvent was removed under reduced pressure. The crude product was dissolved in CH$_2$Cl$_2$ (30 mL), and the organic layer was washed with a saturated solution of NaHCO$_3$ (2 × 10 mL). The organic layer was dried over MgSO$_4$ and filtered. The solvent was removed under reduced pressure. The crude product was purified by flash chromatography.

General Procedure B for the Suzuki Cross-Coupling Reaction. To a solution of **2** or **11** (1.0 equiv) in 1,2-dimethoxyethane was added boronic acid or potassium aryltrifluoroborate (1.5 equiv). An aqueous solution (1 M) of potassium carbonate (3.0 equiv) was then injected, and the mixture was degassed by argon bubbling for 15 min. Pd(PPh$_3$)$_4$ (0.05 equiv) was added, and the mixture was heated to 150 °C for 1 h under microwave irradiation. After cooling, the solvent was removed in vacuo. The crude product was purified by flash chromatography.

General Procedure C for the Reduction of Nitro Derivatives. To a solution of the nitro derivative (1 equiv) in ethanol was added tin(II) chloride dihydrate (6.0 equiv). The mixture was refluxed for 12 h. The solvent was removed under reduced pressure followed by the addition of a solution of NaOH (1 M, 100 mL). The crude material was extracted with EtOAc (3 × 60 mL), and the organic layers were washed with water (20 mL). The combined organic layers were dried over MgSO$_4$ and filtered. The solvent was removed under reduced pressure. The crude product was obtained without purification by flash chromatography.

General Procedure D for the Synthesis of Urea Derivatives. A solution of triphosgene (65 mg, 0.22 mmol, 1.0 equiv) in dry THF (10 mL) was cooled to −78 °C. A solution of **4h** or **4i** (3.0 equiv) and *N,N*-diisopropylethylamine (DIPEA; 0.17 mL, 1.04 mmol, 4.8 equiv) in dry THF (5 mL) was added dropwise. The mixture was stirred at −78 °C for 5 min and then warmed to room temperature for 40 min. A solution of amine (3.0 equiv) and DIPEA (85 μL, 0.52 mmol, 2.4

equiv) in dry THF (5 mL) was added dropwise. The solution was stirred at room temperature for 24 h. The reaction was stopped with a saturated solution of NaHCO$_3$ (10 mL). The crude material was extracted with EtOAc (3 × 50 mL). The combined organic layers were dried over MgSO$_4$ and filtered. The solvent was removed under reduced pressure to afford the final product.

General Procedure E for the Cleavage of the MOM Protecting Group. Into a solution of MOM-protected compound (1.0 equiv) in dioxane was injected a solution of HCl in dioxane, 4.0 M (6.0 equiv). The mixture was stirred at room temperature until completion monitored by TLC. The solvent was then removed by filtration and the product washed with diethyl ether.

2-Chloro-4-morpholinopyrido[3,2-*d*]pyrimidine (2a). The reaction was carried out as described for general procedure A using **1** and morpholine. Purification by flash chromatography on silica gel (CH$_2$Cl$_2$/MeOH, 98/2) yielded **2a** as a white solid (223 mg, 89%). Mp: 174−176 °C. ^{1}H NMR (400 MHz, CDCl$_3$): δ 3.87 (t, *J* = 5.0 Hz, 4H), 4.57 (br s, 4H), 7.59 (dd, *J* = 4.2 Hz, *J* = 8.5 Hz, 1H) 8.02 (dd, *J* = 1.7 Hz, *J* = 8.5 Hz, 1H), 8.67 (dd, *J* = 1.7 Hz, *J* = 4.2 Hz, 1H). HRMS (EI/MS): *m/z* calcd for C$_{11}$H$_{11}$ClN$_4$O [M + H]$^+$ 251.0621, found 251.0700.

2-Chloro-4-thiomorpholinopyrido[3,2-*d*]pyrimidine (2b). The reaction was carried out as described for general procedure A using **1** and thiomorpholine. Purification by flash chromatography on silica gel (petroleum ether/EtOAc, 9/1) yielded **2b** as a yellow solid (201 mg, 75%). Mp: 166−168 °C. NMR ^{1}H (400 MHz, CDCl$_3$): δ 2.80 (t, *J* = 8.0 Hz, 4H), 4.71 (br s, 4H), 7.54 (dd, *J* = 4.1 Hz, *J* = 8.5 Hz, 1H), 8.00 (dd, *J* = 1.7 Hz, *J* = 8.5 Hz, 1H), 8.63 (dd, *J* = 1.7 Hz, *J* = 4.1 Hz, 1H). HRMS (EI/MS): *m/z* calcd for C$_{11}$H$_{11}$ClN$_4$S [M + H]$^+$ 267.0393, found 267.0469.

2-Chloro-4-(1,1-dioxothiomorpholino)pyrido[3,2-*d*]-pyrimidine (2c). The reaction was carried out as described for general procedure A using **1** and thiomorpholine 1,1-dioxide. Purification by flash chromatography on silica gel (CH$_2$Cl$_2$/MeOH, 98/2) yielded **2c** as a white solid (174 mg, 58%). Mp: 250 °C. ^{1}H NMR (400 MHz, (CD$_3$)$_2$SO): δ 3.40 (s, 4H), 4.82 (br s, 4H), 7.87 (dd, *J* = 4.2 Hz, *J* = 8.5 Hz, 1H), 8.14 (d, *J* = 8.5 Hz, 1H), 8.84 (d, *J* = 4.2 Hz, 1H). HRMS (EI/MS): *m/z* calcd for C$_{11}$H$_{11}$ClN$_4$O$_2$S [M + H]$^+$ 299.0291, found 299.0372.

2-Chloro-4-(4-methylpiperazin-1-yl)pyrido[3,2-*d*]pyrimidine (2d). The reaction was carried out as described for general procedure A using **1** and 1-methylpiperazine. Purification by flash chromatography on silica gel (CH$_2$Cl$_2$/MeOH, 99/1) yielded **2d** as a yellow solid (224 mg, 85%). Mp: 111−113 °C. ^{1}H NMR (400 MHz, CDCl$_3$): δ 2.35 (s, 3H), 2.59 (br s, 4H), 4.55 (br s, 4H), 7.58 (dd, *J* = 4.1 Hz, *J* = 8.5 Hz, 1H), 8.00 (dd, *J* = 1.7 Hz, *J* = 8.5 Hz, 1H), 8.67 (dd, *J* = 1.7 Hz, *J* = 4.1 Hz, 1H). HRMS (EI/MS): *m/z* calcd for C$_{12}$H$_{14}$ClN$_5$ [M + H]$^+$ 264.0938, found 264.1021.

2-Chloro-4-(4,4-difluoropiperidin-1-yl)pyrido[3,2-*d*]-pyrimidine (2e). The reaction was carried out as described for general procedure A using **1** and 4,4-difluoropiperidine. Purification by flash chromatography on silica gel (CH$_2$Cl$_2$/MeOH, 99/1) yielded **2e** as a yellow solid (228 mg, 80%). Mp: 136−138 °C. ^{1}H NMR (400 MHz, CDCl$_3$): δ 2.18 (m, 4H), 4.62 (br s, 4H), 7.63 (dd, *J* = 4.1 Hz, *J* = 8.5 Hz, 1H), 8.05 (dd, *J* = 1.7 Hz, *J* = 8.5 Hz, 1H), 8.71 (dd, *J* = 1.7 Hz, *J* = 4.1 Hz, 1H). HRMS (EI/MS): *m/z* calcd for C$_{12}$H$_{11}$ClF$_2$N$_4$ [M + H]$^+$ 285.0640, found 285.0725.

2-Chloro-4-((3-pyridylmethyl)amino)pyrido[3,2-*d*]-pyrimidine (2f). The reaction was carried out as described for general procedure A using **1** and 3-picolylamine. Purification by flash chromatography on silica gel (CH$_2$Cl$_2$/MeOH, 99/1) yielded **2f** as a white solid (0.152 mg, 61%). Mp: 154−156 °C. ^{1}H NMR (400 MHz, (CD$_3$)$_2$SO): δ 4.73 (d, *J* = 6.4 Hz, 2H), 7.35 (dd, *J* = 7.8 Hz, *J* = 4.8 Hz, 1H), 7.87 (m, 2H), 8.07 (dd, *J* = 8.5 Hz, *J* = 1.4 Hz, 1H), 8.49 (m, 1H), 8.62 (s, 1H), 8.82 (dd, *J* = 4.2 Hz, *J* = 1.3 Hz, 1H), 9.67 (t, *J* = 6.3 Hz, 1H). HRMS (EI/MS): *m/z* calcd for C$_{13}$H$_{15}$ClN$_4$O [M + H]$^+$ 272.0621, found 279.0636.

2-Chloro-4-((2*R*,6*R*)-2,6-dimethylmorpholino)pyrido[3,2-*d*]-pyrimidine (2g). The reaction was carried out as described for general procedure A using **1** and (2*R*,6*R*)-2,6-dimethylmorpholine.

Purification by flash chromatography on silica gel (petroleum ether/EtOAc, 15/85) yielded **2g** as a white solid (243 mg, 87%). Mp: 158−160 °C. ^{1}H NMR (400 MHz, CDCl$_3$): δ 1.28 (s, 3H), 1.31 (s, 3H), 2.88 (m, 2H), 3.78 (dqd, *J* = 2.4 Hz, *J* = 6.2 Hz, *J* = 12.5 Hz, 2H), 5.35 (s, 1H), 6.19 (s, 1H), 7.59 (dd, *J* = 4.2 Hz, *J* = 8.5 Hz, 1H), 8.02 (dd, *J* = 4.2 Hz, *J* = 8.5 Hz, 1H), 8.69 (dd, *J* = 1.7 Hz, *J* = 4.2 Hz, 1H). HRMS (EI/MS): *m/z* calcd for C$_{13}$H$_{15}$ClN$_4$O [M + H]$^+$ 279.0934, found 279.1008.

2-(3-Hydroxyphenyl)-4-morpholinopyrido[3,2-*d*]pyrimidine (3a). The reaction was carried out as described for general procedure B using **2a** (200 mg, 0.798 mmol) and 3-hydroxyphenylboronic acid (132 mg, 0.958 mmol). Purification by flash chromatography on silica gel (petroleum ether/EtOAc, 8/2) yielded **3a** as a white solid (173 mg, 76%). Mp: 236−238 °C. ^{1}H NMR (400 MHz, (CD$_3$)$_2$SO): δ 3.81 (m, 4H), 4.51 (br s, 4H), 6.89 (m, 1H), 7.29 (dd, *J* = 4.0 Hz, *J* = 8.3 Hz, 1H), 7.80 (m, 1H), 7.89 (m, 2H), 8.17 (dd, *J* = 1.5 Hz, *J* = 8.3 Hz, 1H), 8.77 (d, *J* = 7.8 Hz, 1H), 9.54 (m, 1H). HRMS (EI/MS): *m/z* calcd for C$_{17}$H$_{16}$N$_4$O$_2$ [M + H]$^+$ 309.1273, found 309.1364. Purity: >96% by HPLC, t_R = 6.47 min.

2-(3-Hydroxyphenyl)-4-thiomorpholinopyrido[3,2-*d*]-pyrimidine (3b). The reaction was carried out as described for general procedure B using **2b** (180 mg, 0.675 mmol) and 3-hydroxyphenylboronic acid (124 mg, 0.810 mmol). Purification by flash chromatography on silica gel (CH$_2$Cl$_2$/MeOH, 96/4) yielded **3b** as a white solid (167 mg, 76%). Mp: 238−240 °C. ^{1}H NMR (400 MHz, (CD$_3$)$_2$SO): δ 2.85 (br s, 4H), 4.75 (br s, 4H), 6.90 (m, 1H), 7.28 (t, *J* = 7.5 Hz, 1H), 7.78 (dd, *J* = 5.0 Hz, *J* = 10.0 Hz, 1H), 7.88 (m, 2H), 8.17 (dd, *J* = 2.5 Hz, *J* = 10.0 Hz, 1H), 8.76 (dd, *J* = 2.5 Hz, *J* = 5.0 Hz, 1H), 9.55 (s, 1H). HRMS (EI/MS): *m/z* calcd for C$_{17}$H$_{16}$N$_4$OS [M + H]$^+$ 325.1045, found 325.1113. Purity: >97% by HPLC, t_R = 7.75 min.

2-(3-Hydroxyphenyl)-4-(1,1-dioxothiomorpholino)pyrido-[3,2-*d*]pyrimidine (3c). The reaction was carried out as described for general procedure B using **2c** (160 mg, 0.536 mmol) and 3-hydroxyphenylboronic acid (89 mg, 0.643 mmol). Purification by flash chromatography on silica gel (CH$_2$Cl$_2$/MeOH, 98/2) yielded **3c** as a white solid (162 mg, 85%). Mp: 219−221 °C. ^{1}H NMR (400 MHz, (CD$_3$)$_2$SO): δ 3.41 (br s, 4H), 4.90 (br s, 4H), 6.90 (d, *J* = 8.0 Hz, 1H), 7.31 (t, *J* = 8.0 Hz, 1H), 7.86 (dd, *J* = 4.1 Hz, *J* = 8.5 Hz, 1H), 7.91 (m, 2H), 8.22 (dd, *J* = 1.6 Hz, *J* = 8.5 Hz, 1H), 8.81 (dd, *J* = 1.6 Hz, *J* = 4.1 Hz, 1H), 9.58 (s, 1H). HRMS (EI/MS): *m/z* calcd for C$_{17}$H$_{16}$N$_4$O$_3$S [M + H]$^+$ 357.0943, found 357.1018. Purity: >97% by HPLC, t_R = 7.37 min.

2-(3-Hydroxyphenyl)-4-(4-methylpiperazin-1-yl)pyrido[3,2-*d*]pyrimidine (3d). The reaction was carried out as described for general procedure B using **2d** (200 mg, 0.758 mmol) and 3-hydroxyphenylboronic acid (126 mg, 0.910 mmol). Purification by flash chromatography on silica gel (CH$_2$Cl$_2$/MeOH, 99/1) yielded **3d** as a yellow solid (211 mg, 87%). Mp: 174−176 °C. ^{1}H NMR (400 MHz, CDCl$_3$): δ 2.60 (s, 3H), 2.96 (br s, 4H), 4.90 (br s, 4H), 7.15 (d, *J* = 8.0 Hz, 1H), 7.35 (br, 1H), 7.53 (t, *J* = 8.0 Hz, 1H), 7.79 (dd, *J* = 4.1 Hz, *J* = 8.5 Hz, 1H), 8.13 (m, 1H), 8.24 (dd, *J* = 1.6 Hz, *J* = 8.5 Hz, 1H), 8.34 (dd, *J* = 1.6 Hz, *J* = 4.1 Hz, 1H), 8.88 (m, 1H). HRMS (EI/MS): *m/z* calcd for C$_{18}$H$_{19}$N$_5$O [M + H]$^+$ 322.1590, found 322.1682 Purity: >96% by HPLC, t_R = 4.82 min.

4-(4,4-Difluoropiperidin-1-yl)-2-(3-hydroxyphenyl)pyrido-[3,2-*d*]pyrimidine (3e). The reaction was carried out as described for general procedure B using **2e** (200 mg, 0.703 mmol) and 3-hydroxyphenylboronic acid (116 mg, 0.844 mmol). Purification by flash chromatography on silica gel (CH$_2$Cl$_2$/MeOH, 99/1) yielded **3e** as a yellow solid (147 mg, 61%). Mp: 175 °C. ^{1}H NMR (400 MHz, CDCl$_3$): δ 2.20 (m, 4H), 4.65 (s, 4H), 5.91 (br s, OH), 6.96 (d, *J* = 7.8 Hz, 1H), 7.35 (t, *J* = 7.8 Hz, 1H), 7.62 (dd, *J* = 4.1 Hz, *J* = 8.5 Hz, 1H), 7.99 (s, 1H), 8.04 (d, *J* = 7.8 Hz, 1H), 8.21 (dd, *J* = 2.6 Hz, *J* = 8.5 Hz, 1H), 8.70 (dd, *J* = 2.6 Hz, *J* = 4.1 Hz, 1H). HRMS (EI/MS): *m/z* calcd for C$_{18}$H$_{16}$F$_2$N$_4$O [M + H]$^+$ 343.1292, found 343.1364. Purity: >96% by HPLC, t_R = 8.47 min.

4-((2*R*,6*R*)-2,6-Dimethylmorpholino)-2-(3-hydroxyphenyl)-pyrido[3,2-*d*]pyrimidine (3g). The reaction was carried out as described for general procedure B using **2g** (200 mg, 0.718 mmol) and

3-hydroxyphenylboronic acid (119 mg, 0.861 mmol). Purification by flash chromatography on silica gel (CH$_2$Cl$_2$/MeOH, 98/2) yielded **3g** as a white solid (205 mg, 85%). Mp: 219 °C. ^{1}H NMR (400 MHz, CDCl$_3$): δ 1.28 (s, 3H), 1.30 (s, 3H), 2.91 (dd, J = 10.9 Hz, J = 12.9 Hz, 2H), 3.83 (m, 2H), 5.70 (m, 2H), 6.35 (m, 1H), 6.90 (m, 1H), 7.27 (t, J = 7.9 Hz, 1H), 7.51 (dd, J = 4.1 Hz, J = 8.5 Hz, 1H), 7.93 (d, J = 7.8 Hz, 1H), 7.98 (s, 1H), 8.17 (dd, J = 1.6 Hz, J = 8.5 Hz, 1H), 8.63 (dd, J = 1.6 Hz, J = 4.1 Hz, 1H). HRMS (EI/MS): m/z calcd for C$_{19}$H$_{20}$N$_4$O$_2$ [M + H]$^+$ 337.1586, found 337.1661. Purity: >96% by HPLC, t_R = 7.50 min.

2-(2-Hydroxyphenyl)-4-morpholinopyrido[3,2-*d*]pyrimidine (4a). The reaction was carried out as described for general procedure B using **2a** (200 mg, 0.798 mmol) and 2-hydroxyphenylboronic acid (132 mg, 0.958 mmol). Purification by flash chromatography on silica gel (petroleum ether/EtOAc, 7/3) yielded **4a** as a yellow solid (215 mg, 87%). Mp: 173−175 °C. ^{1}H NMR (400 MHz, CDCl$_3$): δ 3.94 (t, J = 5.0 Hz, 4H), 4.63 (br s, 4H), 6.90 (dd, J = 7.2 Hz, J = 8.0 Hz, 1H), 7.02 (d, J = 8.0 Hz, 1H), 7.37 (t, J = 7.2 Hz, 1H), 7.61 (dd, J = 4.0 Hz, J = 4.4 Hz, 1H), 8.06 (d, J = 8.0 Hz, 1H), 8.41 (dd, J = 2.5 Hz, J = 10.0 Hz, 1H), 8.66 (dd, J = 2.5 Hz, J = 5.0 Hz, 1H), 14.3 (s, 1H). HRMS (EI/MS): m/z calcd for C$_{17}$H$_{16}$N$_4$O$_2$ [M + H]$^+$ 309.1273, found 309.1363. Purity: >98% by HPLC, t_R = 11.84 min.

2-(4-Hydroxyphenyl)-4-morpholinopyrido[3,2-*d*]pyrimidine (4b). The reaction was carried out as described for general procedure B using **2a** (200 mg, 0.798 mmol) and 4-hydroxyphenylboronic acid (132 mg, 0.958 mmol). Purification by flash chromatography on silica gel (petroleum ether/EtOAc, 7/3) yielded **4b** as a white solid (182 mg, 74%). Mp: 252−254 °C. ^{1}H NMR (400 MHz, (CD$_3$)$_2$SO): δ 3.81 (t, J = 5.2 Hz, 4H), 4.48 (br s, 4H), 6.80 (m, 2H), 7.74 (m, 1H), 8.25 (m, 1H), 8.28 (m, 2H), 8.70 (m, 1H). HRMS (EI/MS): m/z calcd for C$_{17}$H$_{16}$N$_4$O$_2$ [M + H]$^+$ 309.1273, found 309.1352. Purity: >98% by HPLC, t_R = 6.25 min.

2-(3-Methoxyphenyl)-4-morpholinopyrido[3,2-*d*]pyrimidine (4c). The reaction was carried out as described for general procedure B using **2a** (200 mg, 0.798 mmol) and 3-methoxyphenylboronic acid (146 mg, 0.957 mmol). Purification by flash chromatography on silica gel (petroleum ether/EtOAc, 2/8) yielded **4c** as a white solid (219 mg, 85%). Mp: 118−120 °C. ^{1}H NMR (400 MHz, CDCl$_3$): δ 3.93 (s, 4H), 3.95 (s, 3H), 4.60 (br s, 4H), 7.03 (dd, J = 2.6 Hz, J = 8.1 Hz, 1H), 7.40 (tJ = 7.9 Hz,, 1H), 7.61 (dd, J = 4.1 Hz, J = 8.5 Hz, 1H), 8.08 (dd, J = 5.1 Hz, J = 13.3 Hz, 2H), 8.19 (dd, J = 1.7 Hz, J = 8.5 Hz, 1H), 8.68 (dd, J = 1.7 Hz, J = 4.1 Hz, 1H). HRMS (EI/MS): m/z calcd for C$_{18}$H$_{18}$N$_4$O$_2$ [M + H]$^+$ 323.1616, found 323.1504. Purity: >97% by HPLC, t_R = 7.97 min.

2-(4-Methoxyphenyl)-4-morpholinopyrido[3,2-*d*]pyrimidine (4d). The reaction was carried out as described for general procedure B using **2a** (200 mg, 0.798 mmol) and 4-methoxyphenylboronic acid (146 mg, 0.958 mmol). Purification by flash chromatography on silica gel (petroleum ether/EtOAc, 7/3) yielded **4d** as a white solid (196 mg, 76%). Mp: 178−180 °C^{1}H NMR (400 MHz, CDCl$_3$): δ 3.88 (s, 3H), 3.92 (t, J = 5.0 Hz, 4H), 4.58 (m, 4H), 6.99 (d, J = 9.0 Hz, 2H), 7.58 (dd, J = 4.2 Hz, J = 8.5 Hz, 1H), 8.14 (dd, J = 1.7 Hz, J = 8.5 Hz, 1H), 8.45 (d, J = 9.0 Hz, 2H), 8.63 (dd, J = 1.7 Hz, J = 4.2 Hz, 1H). HRMS (EI/MS): m/z calcd for C$_{18}$H$_{18}$N$_4$O$_2$ [M + H]$^+$ 323.1616, found 323.1504. Purity: >97% by HPLC, t_R = 7.13 min.

2-(3-(Hydroxymethyl)phenyl)-4-morpholinopyrido[3,2-*d*]-pyrimidine (4e). The reaction was carried out as described for general procedure B using **2a** (200 mg, 0.798 mmol) and 3-(hydroxymethyl)phenylboronic acid (146 mg, 0.958 mmol). Purification by flash chromatography on silica gel (petroleum ether/EtOAc, 8/2) yielded **4e** as a yellow solid (226 mg, 88%). Mp: 119−121 °C. ^{1}H NMR (400 MHz, CDCl$_3$): δ 3.92 (t, J = 6.0 Hz, 4H), 4.59 (br s, 4H), 4.78 (s, 2H), 7.45 (m, 2H), 7.60 (dd, J = 4.0 Hz, J = 8.0 Hz, 1H), 7.65 (m, 1H), 8.17 (m, 1H), 8.38 (dd, J = 2.0 Hz, J = 8.0 Hz, 1H), 8.45 (m, 1H), 8.66 (dd, J = 2.0 Hz, J = 4.0 Hz, 1H). HRMS (EI/MS): m/z calcd for C$_{18}$H$_{18}$N$_4$O$_2$ [M + H]$^+$ 323.1430, found 323.1498. Purity: >97% by HPLC, t_R = 6.17 min.

2-(4-(Hydroxymethyl)phenyl)-4-morpholinopyrido[3,2-*d*]-pyrimidine (4f). The reaction was carried out as described for general procedure B using **2a** (200 mg, 0.798 mmol) and 4-(hydroxymethyl)-phenylboronic acid (146 mg, 0.958 mmol). Purification by flash chromatography on silica gel (petroleum ether/EtOAc, 8/2) yielded **4f** as a white solid (183 mg, 71%). Mp: 221−223 °C. ^{1}H NMR (400 MHz, CDCl$_3$): δ 3.93 (m, 4H), 4.60 (br s, 4H), 4.77 (s, 2H), 7.46 (d, J = 8.1 Hz, 2H), 7.60 (dd, J = 4.1 Hz, J = 8.5 Hz, 1H), 8.18 (dd, J = 1.7 Hz, J = 8.5 Hz, 1H), 8.47 (d, J = 8.2 Hz, 2H), 8.67 (dd, J = 1.7 Hz, J = 4.1 Hz, 1H). HRMS (EI/MS): m/z calcd for C$_{18}$H$_{18}$N$_4$O$_2$ [M + H]$^+$ 323.1430, found 323.1512. Purity: >99% by HPLC, t_R = 6.10 min.

2-(3-Aminophenyl)-4-morpholinopyrido[3,2-*d*]pyrimidine (4g). The reaction was carried out as described for general procedure B using **2a** (200 mg, 0.798 mmol, 1.0 equiv) and 3-nitrophenylboronic acid (161 mg, 0.958 mmol, 1.2 equiv). Purification by flash chromatography on silica gel (petroleum ether/EtOAc, 85/15) yielded the nitro derivative as a yellow solid (191 mg, 71%). Mp: 193−195 °C. ^{1}H NMR (400 MHz, (CD$_3$)$_2$SO): δ 3.84 (m, 4H), 4.56 (br s, 4H), 7.83 (m, 2H), 8.27 (dd, J = 1.4 Hz, J = 8.5 Hz, 1H), 8.36 (dd, J = 4.0 Hz, J = 8.5 Hz, 1H), 8.81 (dd, J = 1.4 Hz, J = 4.0 Hz, 1H), 8.85 (d, J = 7.8 Hz, 1H), 9.16 (s, 1H). HRMS (EI/MS): m/z calcd for C$_{17}$H$_{15}$N$_5$O$_3$ [M + H]$^+$ 338.1175, found 338.1250. Then the reduction of the nitro group was carried out as described for general procedure C using the nitro derivative (180 mg, 0.534 mmol, 1.0 equiv). The crude product was obtained without purification by flash chromatography to afford **4g** as a white solid (131 mg, 80%). Mp: 182−184 °C. ^{1}H NMR (400 MHz, (CD$_3$)$_2$SO): δ 3.82 (m, 4H), 4.51 (br s, 4H), 5.45 (br, 2H), 6.70 (dd, J = 1.4 Hz, J = 7.8 Hz, 1H), 7.13 (t, J = 7.8 Hz, 1H), 7.63 (d, J = 7.7 Hz, 1H), 7.72 (s, 1H), 7.77 (dd, J = 4.1 Hz, J = 8.5 Hz, 1H), 8.15 (dd, J = 1.4 Hz, J = 8.5 Hz, 1H), 8.74 (dd, J = 1.4 Hz, J = 4.0 Hz, 1H). HRMS (EI/MS): m/z calcd for C$_{17}$H$_{17}$N$_5$O [M + H]$^+$ 308.1433, found 308.1507. Purity: >99% by HPLC, t_R = 5.97 min.

2-(4-Aminophenyl)-4-morpholinopyrido[3,2-*d*]pyrimidine 4h. The reaction was carried out as described for general procedure B using **2a** (200 mg, 0.798 mmol, 1.0 equiv) and 4-nitrophenylboronic acid (161 mg, 0.958 mmol, 1.2 equiv). Purification by flash chromatography on silica gel (CH$_2$Cl$_2$/petroleum ether, 8/2) yielded the nitro derivative as a yellow solid (234 mg, 87%). Mp: 211−213 °C. ^{1}H NMR (400 MHz, CDCl$_3$): δ 3.82 (m, 4H), 4.63 (br s, 4H), 7.66 (dd, J = 4.1 Hz, J = 8.5 Hz, 1H), 8.20 (dd, J = 1.7 Hz, J = 8.5 Hz, 1H), 8.32 (d, J = 8.9 Hz, 2H), 8.66 (d, J = 8.0 Hz, 2H), 8.73 (dd, J = 1.7 Hz, J = 4.1 Hz, 1H). HRMS (EI/MS): m/z calcd for C$_{17}$H$_{15}$N$_5$O$_3$ [M + H]$^+$ 338.1175, found 338.1257. Then the reduction of the nitro group was carried out as described for general procedure C using the nitro derivative (600 mg, 1.78 mmol, 1.0 equiv) The crude product was obtained without purification by flash chromatography to afford **4h** as a white solid (443 mg, 80%). Mp: 221−223 °C. ^{1}H NMR (400 MHz, CDCl$_3$): δ 1.62 (br, 2H), 3.93 (m, 4H), 4.56 (br s, 4H), 6.75 (d, J = 8.7 Hz, 2H), 7.56 (dd, J = 4.1 Hz, J = 8.5 Hz, 1H), 8.12 (dd, J = 1.6 Hz, J = 8.5 Hz, 1H), 8.33 (d, J = 8.7 Hz, 2H), 8.61 (dd, J = 1.7 Hz, J = 4.1 Hz, 1H). HRMS (EI/MS): m/z calcd for C$_{17}$H$_{17}$N$_5$O [M + H]$^+$ 308.1433, found 308.1509. Purity: >96% by HPLC, t_R = 6.29 min.

4-Morpholino-2-(3-pyridyl)pyrido[3,2-*d*]pyrimidine (4i). The reaction was carried out as described for general procedure B using **2a** (200 mg, 0.798 mmol) and 3-pyridineboronic acid (118 mg, 0.958 mmol). Purification by flash chromatography on silica gel (CH$_2$Cl$_2$/MeOH, 99/1) yielded **4i** as a yellow solid (178 mg, 76%). Mp: 159−161 °C. ^{1}H NMR (400 MHz, CDCl$_3$): δ 3.92 (t, J = 6.0 Hz, 4H), 4.63 (br s, 4H), 7.61−7.89 (m, 4H), 8.20 (dd, J = 1.75 Hz, J = 8.5 Hz, 1H), 8.31 (dd, J = 1.5 Hz, J = 6.25 Hz, 1H), 8.73 (dd, J = 1.5 Hz, J = 6.25 Hz, 1H). HRMS (EI/MS): m/z calcd for C$_{16}$H$_{15}$N$_5$O [M + H]$^+$ 294.1277, found 294.1359. Purity: >95% by HPLC, t_R = 6.48 min.

2-(1*H*-Indazol-6-yl)-4-morpholinopyrido[3,2-*d*]pyrimidine (4j). The reaction was carried out as described for general procedure B using **2a** (200 mg, 0.798 mmol) and potassium 1*H*-indazole-6-trifluoroborate (155 mg, 0.958 mmol). Purification by flash chromatography on silica gel (petroleum ether/EtOAc, 8/2) yielded **4j** as a white solid (119 mg, 45%). Mp: 236−238 °C. ^{1}H NMR (400 MHz, CDCl$_3$): δ 3.97 (s, 4H), 4.56 (br s, 4H), 7.55 (d, J = 8.1 Hz, 2H), 7.53 (m, 1H), 8.20 (d, J = 8.8 Hz, 2H), 8.62 (d, J = 8.1 Hz, 2H), 8.67 (m, 1H), 8.97 (s, 1H), 10.31 (bd, 1H). HRMS (EI/MS): m/z calcd for C$_{18}$H$_{16}$N$_6$O [M + H]$^+$ 333.1386, found 333.1451. Purity: >98% by HPLC, t_R = 6.26 min.

2-(1H-Indazol-4-yl)-4-morpholinopyrido[3,2-d]pyrimidine (4k). The reaction was carried out as described for general procedure B using **2a** (200 mg, 0.798 mmol) and potassium 1H-indazole-4-trifluoroborate (191 mg, 0.957 mmol). Purification by flash chromatography on silica gel (CH$_2$Cl$_2$/MeOH, 98/2) yielded **4k** as a white solid (129 mg, 49%). Mp: 212−214 °C. ^{1}H NMR (400 MHz, (CD$_3$)$_2$SO): δ 3.77−3.91 (m, 4H), 4.54 (br s, 4H), 7.50 (t, J = 7.8 Hz, 1H), 7.71 (d, J = 8.2 Hz, 1H), 7.84 (dd, J = 4.1 Hz, J = 8.5 Hz, 1H), 8.29 (d, J = 7.2 Hz, 1H), 8.35 (dd, J = 1.6 Hz, J = 8.5 Hz, 1H), 8.80 (dd, J = 1.6 Hz, J = 4.1 Hz, 1H), 9.01 (s, 1H), 13.22 (s, 1H). HRMS (EI/MS): m/z calcd for C$_{18}$H$_{16}$N$_6$O [M + H]$^+$ 333.1458, found 333.1460. Purity: >99% by HPLC, t_R = 6.80 min.

2-(2-Aminopyridyl)-4-morpholinopyrido[3,2-d]pyrimidine (4l). The reaction was carried out as described for general procedure B using **2a** (200 mg, 0.798 mmol) and potassium 2-aminopyridine-5-trifluoroborate (211 mg, 0.958 mmol). Purification by flash chromatography on silica gel (CH$_2$Cl$_2$/MeOH, 96/4) yielded **4l** as a yellow solid (71 mg, 23%). Mp: 242−244 °C. ^{1}H NMR (400 MHz, CDCl$_3$): δ 3.92 (m, 4H), 4.61 (br s, 4H), 4.73 (br s, 2H), 6.57 (dd, J = 8.6 Hz, J = 0.8 Hz, 1H), 7.57 (dd, J = 8.5 Hz, J = 4.1 Hz, 1H), 8.10 (dd, J = 8.5 Hz, J = 1.7 Hz, 1H), 8.53 (dd, J = 8.6 Hz, J = 2.3 Hz, 1H), 8.63 (dd, J = 4.1 Hz, J = 1.7 Hz, 1H), 9.19 (dd, J = 2.3 Hz, J = 0.7 Hz, 1H) . HRMS (EI/MS): m/z calcd for C$_{16}$H$_{16}$N$_6$O [M + H]$^+$ 309.1458, found 309.1460. Purity: >97% by HPLC, t_R = 5.76 min.

2-(2-Aminopyrimidinyl)-4-morpholinopyrido[3,2-d]pyrimidine (4m). The reaction was carried out as described for general procedure B using **2a** (200 mg, 0.798 mmol) and potassium 2-aminopyrimidine-5- trifluoroborate (212 mg, 0.958 mmol). Purification by flash chromatography on silica gel (CH$_2$Cl$_2$/MeOH, 96/4) yielded **4m** as a white solid (178 mg, 72%). Mp: 260 °C. ^{1}H NMR (400 MHz, CDCl$_3$): δ 3.92 (m, 4H), 4.58 (br s, 4H), 5.30 (m, 2H), 7.59 (dd, J = 4.0 Hz, J = 8.5 Hz, 1H), 8.11 (d, J = 4.0 Hz, J = 8.5 Hz, 1H), 8.65 (d, J = 4.0 Hz, 1H), 9.33 (s, 2H). HRMS (EI/MS): m/z calcd for C$_{15}$H$_{15}$N$_7$O [M + H]$^+$ 310.1338, found 310.1403. Purity: >98% by HPLC, t_R = 5.75 min.

4-Morpholino-2-(2-(acetylamino)pyrimidinyl)pyrido[3,2-d]pyrimidine (5). To a solution of **4m** (125 mg, 0.404 mmol, 1.0 equiv) in dimethylformamide (DMF; 2 mL) was added acetic anhydride (0.38 mL, 4.04 mmol, 10.0 equiv). The mixture was heated at 120 °C for 30 min under microwave irradiation. After cooling, the crude material was then diluted in water (30 mL) and extracted with EtOAc (5 mL). The combined organic layers were washed with water (2 × 30 mL) and dried over MgSO$_4$. The solvent was removed in vacuo, and purification by flash chromatography on silica gel (CH$_2$Cl$_2$/MeOH, 98/2) yielded **5** as a white solid (40 mg, 28%). Mp: 260−262 °C. ^{1}H NMR (400 MHz, CDCl$_3$): δ 2.56 (d, J = 4.7 Hz, 3H), 3.92 (d, J = 3.9 Hz, 4H), 4.60 (br s, 4H), 7.63 (m, 1H), 8.15 (s, 1H), 8.52 (s, 1H), 8.69 (s, 1H), 9.57 (d, J = 5.2 Hz, 2H). HRMS (EI/MS): m/z calcd for C$_{17}$H$_{17}$N$_7$O$_2$ [M + H]$^+$ 352.1444, found 352.1505. Purity: >99% by HPLC, t_R = 6.69 min.

4-Morpholino-2-(2-(diacetylamino)pyrimidinyl))pyrido[3,2-d]pyrimidine 6. Compound **6** was isolated during the transformation of **4n** into **5** (vide supra) during the purification by flash chromatography on silica gel as a white solid (70 mg, 44%). Mp: 225−227 °C. ^{1}H NMR (400 MHz, CDCl$_3$): δ 2.34 (s, 6H), 3.93 (m, 4H), 4.64 (br s, 4H), 7.68 (dd, J = 4.1 Hz, J = 8.5 Hz, 1H), 8.20 (dd, J = 1.5 Hz, J = 8.5 Hz, 1H), 8.75 (dd, J = 1.5 Hz, J = 4.0 Hz, 1H), 9.79 (s, 2H). HRMS (EI/MS): m/z calcd for C$_{19}$H$_{19}$N$_7$O$_3$ [M + H]$^+$ 394.1549, found 394.1618. Purity: >98% by HPLC, t_R = 9.26 min.

2-Chloro-4-(3-(methoxymethoxy)phenyl)pyrido[3,2-d]pyrimidine (7). To a solution of **1** (300 mg, 1.5 mmol, 1.0 equiv) in dry toluene were added potassium 3-(methoxymethoxy)-phenyltrifluoroborate (256 mg, 1.58 mmol, 1.05 equiv), potassium carbonate (311 mg, 2.25 mmol), and Pd(PPh$_3$)$_4$ (87 mg, 0.08 mmol, 0.05 equiv). The mixture was stirred at 100 °C for 2 h. The solvent was then removed under reduced pressure, and the crude material was dissolved in CH$_2$Cl$_2$ (30 mL). The organic layer was washed with water (2 × 10 mL). The combined organic layers were dried over MgSO$_4$. Purification by flash chromatography on silica gel (petroleum ether/EtOAc, 8/2) yielded **7** as a yellow solid (204 mg, 45%). Mp:

189−191 °C. ^{1}H NMR (400 MHz, CDCl$_3$): δ 3.56 (s, 3H), 5.28 (s, 2H), 6.98 (dd, J = 1.7 Hz, J = 7.2 Hz, 1H), 7.43 (t, J = 7.8 Hz, 1H), 7.56 (dd, J = 4.2 Hz, J = 8.7 Hz, 1H), 7.78 (d, J = 7.8 Hz, 2H), 7.96 (dd, J = 1.6 Hz, J = 8.7 Hz, 1H), 8.63 (dd, J = 1.6 Hz, J = 4.2 Hz, 1H). HRMS (EI-MS): m/z calcd for C$_{15}$H$_{12}$ClN$_3$O$_2$ [M + H]$^+$ 302.1352, found 302.1358.

4-(3-Hydroxyphenyl)-2-morpholinopyrido[3,2-d]pyrimidine (9). To a solution of **7** (150 mg, 0.497 mmol, 1.0 equiv) in dry THF were added successively morpholine (70 µL, 0.746 mmol, 1.5 equiv) and triethylamine (103 µL, 0.746 mmol, 1.5 equiv). The mixture was refluxed for 12 h. The solvent was removed under reduced pressure, and the crude material was dissolved in CH$_2$Cl$_2$ (30 mL). The organic layer was washed with water (2 × 10 mL). The combined organic layers were dried over MgSO$_4$. Purification by flash chromatography on silica gel (petroleum ether/EtOAc, 8/2) yielded the protected **8** as a yellow solid (120 mg, 68%). Direct deprotection of the methoxymethoxy function was directly carried out as described ifor general procedure E (using EtOH as the solvent) to afford **9** as a yellow solid (63 mg, 60%). Mp: 162−164 °C. ^{1}H NMR (400 MHz, CDCl$_3$): δ 3.86 (m, 4H), 4.04 (m, 4H), 6.41 (s, 1H), 7.01 (dd, J = 1.7 Hz, J = 7.2 Hz, 1H), 7.43 (t, J = 8.1 Hz, 1H), 7.56 (dd, J = 4.1 Hz, J = 8.6 Hz, 1H), 7.78 (d, J = 7.8 Hz, 2H), 7.96 (dd, J = 1.6 Hz, J = 8.7 Hz, 1H), 8.63 (dd, J = 1.6 Hz, J = 4.1 Hz, 1H). HRMS (EI/MS): m/z calcd for C$_{17}$H$_{16}$N$_4$O$_2$ [M + H]$^+$ 309.1352, found 309.1358. Purity: >99% by HPLC, t_R = 8.59 min.

2-(3-Hydroxyphenyl)-4-morpholinopyrido[2,3-d]pyrimidine (12a). The reaction was carried out as described for general procedure B using **11** (160 mg, 0.638 mmol) and 3-hydroxyphenylboronic acid (89 mg, 0.643 mmol). Purification by flash chromatography on silica gel (CH$_2$Cl$_2$/MeOH, 99/1) yielded **12a** as a white solid (118 mg, 60%). Mp: > 260 °C. ^{1}H NMR (250 MHz, (CD$_3$)$_2$SO): δ 3.83 (d, J = 4.5 Hz, 4H), 3.89 (d, J = 4.4 Hz, 4H), 6.93 (s, 1H), 7.31 (d, J = 8.0 Hz, 1H), 7.47 (d, J = 4.3 Hz, J = 8.3 Hz, 1H), 7.94 (d, J = 7.6 Hz, 2H), 8.47 (dd, J = 1.7 Hz, J = 8.3 Hz, 1H), 9.01 (dd, J = 1.7 Hz, J = 4.2 Hz, 1H), 9.59 (s, 1H). HRMS (EI/MS): m/z calcd for C$_{17}$H$_{16}$N$_4$O$_2$ [M + H]$^+$ 309.1273, found 309.1364. Purity: >97% by HPLC, t_R = 5.82 min.

2-(3-(Hydroxymethyl)phenyl)-4-morpholinopyrido[2,3-d]pyrimidine (12b). The reaction was carried out as described for general procedure B using **11** (200 mg, 0.798 mmol) and 3-(hydroxymethyl)phenylboronic acid (89 mg, 0.643 mmol). Purification by flash chromatography on silica gel (CH$_2$Cl$_2$/MeOH, 98/2) yielded **12b** as a white solid (167 mg, 65%). Mp: > 260 °C. ^{1}H NMR (400 MHz, (CD$_3$)$_2$SO): δ 3.87−3.78 (m, 4H), 3.97−3.87 (m, 4H), 4.62 (d, J = 3.4 Hz, 2H), 5.32 (s, 1H), 7.47 (dd, J = 3.8 Hz, J = 7.2 Hz, 3H), 8.37 (s, 1H), 8.51−8.45 (m, 2H), 9.02 (dd, J = 1.7 Hz, J = 4.2 Hz, 1H). HRMS (EI/MS): m/z calcd for C$_{18}$H$_{18}$N$_4$O$_2$ [M + H]$^+$ 323.1508, found 323.1514. Purity: >95% by HPLC, t_R = 5.62 min.

2-(2-Aminopyrimidinyl)-4-morpholinopyrido[2,3-d]pyrimidine (12c). The reaction was carried out as described for general procedure B using **11** (200 mg, 0.798 mmol) and potassium 2-aminopyrimidine-5- trifluoroborate (89 mg, 0.643 mmol). Purification by flash chromatography on silica gel (CH$_2$Cl$_2$/MeOH, 98/2) yielded **12c** as a white solid (170 mg, 69%). Mp: > 260 °C. ^{1}H NMR (400 MHz, (CD$_3$)$_2$SO): δ 3.81 (m, 4H), 3.89 (m, 4H), 7.24 (s, 2H), 7.42 (dd, J = 4.3 Hz, J = 8.2 Hz, 1H), 8.43 (dd, J = 1.5 Hz, J = 8.2 Hz, 1H), 8.99−8.93 (dd, J = 1.5 Hz, J = 4.3 Hz, 1H), 9.20 (s, 2H). HRMS (EI/MS): m/z calcd for C$_{15}$H$_{15}$N$_7$O [M + H]$^+$ 310.1416, found 310.1423. Purity: >99% by HPLC, t_R = 4.87 min.

2-(4-(1-Methyl-3-phenylurea))-4-morpholinopyrido[3,2-d]pyrimidine (13a). The reaction was carried out as described for general procedure D using **4h** (200 mg, 0.651 mmol) and methylamine (22 µL, 0.651 mmol). The crude product was obtained without purification by flash chromatography to afford **13a** as a yellow solid (50 mg, 21%). Mp: 223−225 °C. ^{1}H NMR (400 MHz, (CD$_3$)$_2$CO): δ 2.83 (br s, 3H), 3.87 (m, 4H), 4.57 (br s, 4H), 5.68 (br s, 1H), 7.47 (d, J = 8.8 Hz, 2H), 7.58 (dd, J = 4.1 Hz, J = 8.5 Hz, 1H), 8.00 (dd, J = 1.7 Hz, J = 8.5 Hz, 1H), 8.14 (br s, 1H), 8.30 (d, J = 8.8 Hz, 2H), 8.57 (dd, J = 1.7 Hz, J = 4.1 Hz, 1H). HRMS (EI/MS): m/z calcd for C$_{19}$H$_{20}$N$_6$O$_2$ [M + H]$^+$ 365.1648, found 365.1717. Purity: >96% by HPLC, t_R = 6.19 min.

2-(4-(1-(3-(Hydroxymethyl)phenyl)-3-phenylurea))-4-morpholinopyrido[3,2-d]pyrimidine (13b). The reaction was carried out as described for general procedure D using **4h** (100 mg, 0.325 mmol) and (3-aminophenyl)methanol (40 mg, 0.325 mmol). The crude product was obtained without purification by flash chromatography to afford **13b** as a brown solid (59 mg, 40%). Mp: 244−246 °C. ^{1}H NMR (400 MHz, $(CD_3)_2SO$): δ 3.83 (m, 4H), 4.49 (br s, 6H), 5.19 (br s, 1H), 6.94 (d, J = 6.2 Hz, 1H), 7.24 (s, 1H), 7.34 (d, J = 7.1 Hz, 1H), 7.46 (s, 1H), 7.60 (d, J = 7.8 Hz, 2H), 7.79 (s, 1H), 8.16 (d, J = 8.1 Hz, 1H), 8.39 (d, J = 7.7 Hz, 2H), 8.73 (br s, 2H), 8.92 (s, 1H). HRMS (EI/MS): m/z calcd for $C_{25}H_{24}N_6O_3$ [M + H]$^+$ 457.1477, found 457.1985. Purity: >95% by HPLC, t_R = 6.98 min.

2-(4-(1-(4-(Hydroxymethyl)phenyl)-3-phenylurea))-4-morpholinopyrido[3,2-d]pyrimidine (13c). The reaction was carried out as described for general procedure D using **4h** (65 mg, 0.211 mmol) and (4-aminophenyl)methanol (26 mg, 0.211 mmol). The crude product was obtained without purification by flash chromatography to afford **13c** as a yellow solid (85 mg, 89%). Mp: 220−222 °C. ^{1}H NMR (400 MHz, $(CD_3)_2SO$): δ 3.34 (s, 2H), 3.83 (m, 4H), 4.51 (br s, 4H), 5.2 (br s, 1H) 7.22 (d, J = 8.5 Hz, 2H), 7.45 (d, J = 8.5 Hz, 2H), 7.61 (d, J = 8.8 Hz, 2H), 7.78 (dd, J = 4.1 Hz, J = 8.5 Hz, 1H), 8.15 (dd, J = 1.6 Hz, J = 8.5 Hz, 1H), 8.37 (d, J = 8.8 Hz, 2H), 8.73 (dd, J = 1.6 Hz, J = 4.1 Hz, 1H), 9.22 (s, 1H), 9.45 (s, 1H). HRMS (EI/MS): m/z calcd for $C_{25}H_{24}N_6O_3$ [M + H]$^+$ 457.1477, found 457.1995. Purity: >96% by HPLC, t_R = 6.86 min.

2-(4-(1-(3-Hydroxyphenyl)-3-phenylurea))-4-morpholinopyrido[3,2-d]pyrimidine (13d). The reaction was carried out as described for general procedure D using **4h** (90 mg, 0.293 mmol) and 3-aminophenol (32 mg, 0.293 mmol). The crude product was obtained without purification by flash chromatography to afford **13d** as a brown solid (58 mg, 45%). Mp: 221−223 °C. ^{1}H NMR (400 MHz, $(CD_3)_2SO$): δ 3.83 (d, J = 4.6 Hz, 4H), 4.51 (br s, 4H), 6.39 (dd, J = 2.1 Hz, J = 8.0 Hz, 1H), 6.81 (d, J = 7.7 Hz, 1H), 7.06 (m, 2H), 7.58 (d, J = 8.7 Hz, 2H), 7.78 (dd, J = 4.1 Hz, J = 8.5 Hz, 1H), 8.16 (dd, J = 1.5 Hz, J = 8.5 Hz, 1H), 8.39 (d, J = 8.7 Hz, 2H), 8.63 (s, 1H), 8.73 (dd, J = 1.5 Hz, J = 4.0 Hz, 1H), 8.88 (s, 1H), 9.34 (s, 1H). HRMS (EI/MS): m/z calcd for $C_{24}H_{22}N_6O_3$ [M + H]$^+$ 443.1753, found 443.1827. Purity: >95% by HPLC, t_R = 7.09 min.

2-(4-(1-(4-Hydroxyphenyl)-3-phenylurea))-4-morpholinopyrido[3,2-d]pyrimidine (13e). The reaction was carried out as described for general procedure D using **4h** (120 mg, 0.390 mmol) and 3-aminophenol (43 mg, 0.390 mmol). The crude product was obtained without purification by flash chromatography to afford **13e** as a brown solid (100 mg, 58%). Mp: 239−241 °C. ^{1}H NMR (250 MHz, $(CD_3)_2SO$): δ 3.82 (m, 4H), 4.51 (br s, 4H), 6.70 (m, 2H), 7.24 (m, 2H), 7.57 (d, J = 8.8 Hz, 2H), 7.77 (dd, J = 4.1 Hz, J = 8.5 Hz, 1H), 8.15 (dd, J = 1.7 Hz, J = 8.5 Hz, 1H), 8.38 (m, 3H), 8.72 (dd, J = 1.7 Hz, J = 4.1 Hz, 1H), 8.82 (s, 1H), 9.09 (s, 1H). HRMS (EI/MS): m/z calcd for $C_{24}H_{22}N_6O_3$ [M + H]$^+$ 443.1753, found 443.1826. Purity: >96% by HPLC, t_R = 6.88 min.

4-Morpholino-2-(4-(1-(4-pyridinyl)-3-phenylurea))pyrido-[3,2-d] pyrimidine (13f). The reaction was carried out as described for general procedure D using **4h** (110 mg, 0.358 mmol) and 3-aminopyridine (34 mg, 0.358 mmol). The crude product was obtained without purification by flash chromatography to afford **13f** as a white solid (109 mg, 71%). Mp: > 260 °C. ^{1}H NMR (400 MHz, $(CD_3)_2SO$): δ 3.84 (s, 4H), 4.53 (br s, 4H), 7.48 (d, J = 5.0 Hz, 1H), 7.65 (dd, J = 3.5 Hz, J = 8.0 Hz, 2H), 7.79 (dd, J = 4.0 Hz, J = 8.4 Hz, 1H), 7.97 (m, 1H), 8.19 (d, J = 8.4 Hz, 1H), 8.38 (m, 3H), 8.80−8.71 (m, 2H), 9.73 (br s, 1H), 10.1 (br s, 1H). HRMS (EI/MS): m/z calcd for $C_{23}H_{21}N_7O_2$ [M + H]$^+$ 428.1757, found 428.1828. Purity: >96% by HPLC, t_R = 5.67 min.

4-Morpholino-2-(4-(1-(3-pyridinyl)-3-phenylurea))pyrido-[3,2-d]pyrimidine (13g). The reaction was carried out as described for general procedure D using **4h** (115 mg, 0.374 mmol) and 3-aminopyridine (35 mg, 0.374 mmol). The crude product was obtained without purification by flash chromatography to afford **13g** as a white solid (110 mg, 69%). Mp: 249−251 °C. ^{1}H NMR (400 MHz, $(CD_3)_2SO$): δ 3.97−3.65 (m, 4H), 4.51 (br s, 4H), 7.33 (d, J = 4.7 Hz, 1H), 7.62 (d, J = 8.6 Hz, 2H), 7.78 (m, 1H), 7.97 (d, J = 7.4 Hz, 1H), 8.25−8.10 (m, 2H), 8.38 (d, J = 8.7 Hz, 2H), 8.65 (d, J = 1.7 Hz, 1H), 8.73 (dd, J = 1.6 Hz, J = 4.0 Hz, 1H), 9.61 (s, 1H). HRMS (EI/MS): m/z calcd for $C_{23}H_{21}N_7O_2$ [M + H]$^+$ 428.1757, found 428.1831. Purity: >95% by HPLC, t_R = 5.77 min.

2-(3-(1-(3-(Hydroxymethyl)phenyl)-3-phenylurea))-4-morpholinopyrido[3,2-d]pyrimidine (13h). The reaction was carried out as described for general procedure D using **4g** (65 mg, 0.22 mmol) and (3-aminophenyl)methanol (80 mg, 0.22 mmol). The crude product was obtained without purification by flash chromatography to afford **13h** as a yellow solid (48 mg, 47%). Mp: 230 °C. ^{1}H NMR (400 MHz, $(CD_3)_2SO$): δ 3.83 (m, 4H), 4.42 (d, J = 5.6 Hz, 2H), 4.53 (br s, 4H), 5.05 (t, J = 5.6 Hz, 1H), 7.23 (d, J = 8.5 Hz, 2H), 7.42 (d, J = 8.5 Hz, 2H), 7.71 (d, J = 7.8 Hz, 1H), 7.81 (dd, J = 4.1 Hz, J = 8.5 Hz, 1H), 8.06 (d, J = 7.8 Hz, 1H), 8.20 (dd, J = 1.5 Hz, J = 8.5 Hz, 1H), 8.43 (s, 1H), 8.60 (s, 1H) 8.77 (m, 1H), 8.85 (s, 1H). HRMS (EI/MS): m/z calcd for $C_{25}H_{24}N_6O_3$ [M + H]$^+$ 457.1910, found 457.1988. Purity: >95% by HPLC, t_R = 7.05 min.

Molecular Modeling. *Hardware and Software.* All molecular modeling studies were performed with Schrodinger Molecular Modeling Suite 2010.[49] Maestro was the interface piloting the diverse modules. Glide[38] was used to dock ligands. Calculations were run on a Linux station: Intel Core i7 CPU 950 at 3.07 GHz.

Structure Preparation. The three structures of PI3Kα apo or in complex with wortmannin were retrieved from the Protein Data Bank.[33] Subunit A of each structure, corresponding to the catalytic subunit, was conserved. Structures were aligned and superimposed on their backbone using the Protein Structure Alignment tool of Schrodinger Molecular Modeling Suite 2010. Bond orders and connections of wortmannin were manually corrected, and the ligand was transposed in the two apo structures. Next all three complexes were prepared using the Protein Preparation Wizard workflow of Schrodinger Molecular Modeling Suite 2010. The proteins were subsequently preprocessed (hydrogen atoms added, incomplete residues filled), and an exhaustive sampling was done regarding hydrogen bond assignment. Finally, the hydrogen atoms of the complexes were refined by a minimization stage with a constraint to converge to a structure with an RMSD of 0.3 Å (OPLS2005 force field) to remove steric clashes. The seven cocrystallized inhibitors used as references were extracted from the structures 2X6K, 3LS8, 3L13, 3L16, 3L17, 3DBS, and 3IBE. On the basis of the 3IBE structure of PI3Kγ, the lateral chain of Lys802 in 3HHM was moved by manually modifying the dihedral angles of the residue. The resulting protein model was finally refined by a minimization stage with a constraint to converge to a structure with an RMSD of 0.3 Å (OPLS2005 force field). All docked ligands were built within Marvin.[50] Three-dimensional structures were generated using Corina.[51] Next 3D structures were submitted to the LigPrep module of Schrodinger Molecular Modeling Suite 2010. All ionization states (via the Ionizer module) and tautomers were taken into account at pH 7.0 ± 2.0. The resulting structures were used as the starting point for all docking simulations.

Docking Parameters. The receptor grids were generated using wortmannin as the centroid of the enclosing box, allowing the docking of ligands with a length of 21 Å. Docking calculations were performed with the standard precision of Glide. Ligand flexibility was taken into account, and the option of ring conformation sampling was activated. For each ligand, postdocking minimization was performed on 100 poses, and the 10 best poses were kept and analyzed.

Biological Assays. *In Vitro Kinase Assay on PI3K.* The activity of mTOR was evaluated using a purified protein (ref PV4753 from Invitrogen). The TR-FRET mTOR kinase LANCE Ultra assay kit (Perkin-Elmer) is a fluorescence-based immunoassay for the detection of the phosphorylation of a synthetic peptide, 4EBP1f, a substrate of mTOR. It takes place in 384-well plates and can be divided into two phases: a kinase reaction phase and a phosphorylated peptide detection phase.

In the kinase reaction phase, the following components were mixed in the same well: 5 μL of a solution containing 20 μM ATP and 2 μM PIP2 diluted in kinase assay buffer (50 mM HEPES, pH 7.5, 100 mM NaCl, 0.03% CHAPS, 1 mM EGTA, 3 mM MgCl$_2$, 2 mM DTT), 2.5

μL of kinase at the optimal concentration (222 ng/mL) diluted in kinase assay buffer, and 2.5 μL of serial dilutions of inhibitors diluted in 4% DMSO and kinase assay buffer. For each inhibitor concentration, the assay was run in triplicate. The reaction was then incubated for 60 min at room temperature.

For the ADP detection phase, 5 μL of a detection solution containing europium-labeled anti-ADP antibody (6 nM), Alexa Fluor 647-labeled ADP tracer (12 nM), and EDTA (30 mM, to stop the kinase reaction) diluted in TR-FRET dilution buffer (provided by the manufacturer) was added to the assay well. After 30 min of incubation at room temperature, the 384-well plates were read in a Victor V plate reader configured for HTRF (Perkin-Elmer). Excitation was performed at 340 nm, and emission was measured at 665 and 615 nm. The inhibition curve was then plotted as emission ratio 665 nm/615 nm versus inhibitor concentration.

To calculate substrate conversion values (conversion (%) of ATP in ADP) from the raw TR-FRET emission ratios, an ATP-ADP titration curve was performed with a total nucleotide concentration of 10 μM. The resulting TR-FRET emission ratio was plotted against the conversion of ATP to ADP. The data of this curve were fitted to a three-parameter hyperbolic model with the following equation obtained from the GraphPad Prism software:

$$Y = C + A(1 - (X/(B + X)))$$

The conversion corresponding to each TR-FRET ratio was calculated using the following equation:

$$\text{conversion } (\%) = B\frac{(C + A - \text{ratio})}{\text{ratio} - C}$$

The conversion was then plotted versus the concentration of inhibitor. The amount of inhibitor required to elicit a 50% change in the % conversion of ATP into ADP (the EC50) was then determined. This EC_{50} corresponds to the IC_{50} value of the inhibitor.

In Vitro Kinase Assay on mTOR. The activity of mTOR was evaluated using a purified protein (ref PV4753 from Invitrogen). The TR-FRET mTOR kinase LANCE Ultra assay kit (Perkin-Elmer) is a fluorescence-based immunoassay for the detection of the phosphorylation of a synthetic peptide from 4EBP1, a substrate of mTOR. It takes place in 384-well plates and can be divided into two phases: a kinase reaction phase and a phosphorylated peptide detection phase.

In the kinase reaction phase, the following components were mixed in the same well: 5 μL of a solution containing 10 μM ATP and 50 nM peptide (covalently linked to an acceptor fluorophore, ULight) diluted in kinase assay buffer (50 nM HEPES, pH 7.5, 0.1% Tween 20, 1 mM EGTA, 10 mM MgCl$_2$, 3 mM MnCl$_2$, 2 mM DTT), 2.5 mL of kinase at the optimal concentration (3 ng/μL) diluted in kinase assay buffer, and 5 μL of serial dilutions of inhibitors diluted in 4% DMSO and kinase assay buffer. For each inhibitor concentration, the assay was run in triplicate. The reaction was then incubated for 2 h in a solution containing 32 mM EDTA.

For the detection phase, 5 μL of a detection solution containing europium-labeled antiphosphopeptide antibody (2 nM final concentration) diluted in dilution buffer (provided by the manufacturer) was added to the assay well. After 1 h of incubation at room temperature, the 384-well plates were read in a Victor V plate reader configured for HTRF (Perkin-Elmer). Excitation of europium was performed at 340 nm, and emission of UV light was measured at 665 nm. The inhibition curve was then plotted as the intensity of emission at 665 nm versus the logarithm of the inhibitor concentration.

Kinase Assays. For most assays, kinase-tagged T7 phage strains were grown in parallel in 24-well blocks in an *Escherichia coli* host derived from the BL21 strain. *E. coli* were grown to the log phase and infected with T7 phage from a frozen stock (multiplicity of infection 0.4) and incubated with shaking at 32 °C until lysis (90−150 min). The lysates were centrifuged (6000g) and filtered (0.2 μm) to remove cell debris. The remaining kinases were produced in HEK-293 cells and subsequently tagged with DNA for qPCR detection. Streptavidin-coated magnetic beads were treated with biotinylated small-molecule ligands for 30 min at room temperature to generate affinity resins for

kinase assays. The liganded beads were blocked with excess biotin and washed with blocking buffer (SeaBlock (Pierce), 1% BSA, 0.05% Tween 20, 1 mM DTT) to remove unbound ligand and to reduce nonspecific phage binding. Binding reactions were assembled by combining kinases, liganded affinity beads, and test compounds in 1× binding buffer (20% SeaBlock, 0.17× PBS, 0.05% Tween 20, 6 mM DTT). Test compounds were prepared as 40× stocks in 100% DMSO and directly diluted into the assay. All reactions were performed in polypropylene 384-well plates in a final volume of 0.04 mL. The assay plates were incubated at room temperature with shaking for 1 h, and the affinity beads were washed with wash buffer (1× PBS, 0.05% Tween 20). The beads were then resuspended in elution buffer (1× PBS, 0.05% Tween 20, 0.5 μM nonbiotinylated affinity ligand) and incubated at room temperature with shaking for 30 min. The kinase concentration in the eluates was measured by qPCR.

The compound(s) were screened at the concentration(s) requested, and the results for primary screen binding interactions are reported as "ctrl (%)", where lower numbers indicate stronger hits in the matrix:

$$\text{ctrl (\%) calculation}$$
$$= \frac{\text{test compound signal} - \text{positive control signal}}{\text{negative control signal} - \text{positive control signal}} \times 100$$

Cell Culture and Survival Assay. Skin diploid fibroblast cells were provided by BIOPREDIC International Co. (Rennes, France). HuH7, CaCo-2, and HaCaT cell lines were obtained from the ECACC collection. Cells were grown according to ECACC recommendations. The toxicity test of the compounds on these cells was as follows: A total of 4×10^3 cells/well were seeded in 96-well plates. Twenty-four hours after cell seeding, the cells were exposed to increasing concentrations of the compounds (0.1, 0.3, 0.9, 2.7, 8.3, and 25 μM). After 48 h of treatment, the cells were washed in PBS and fixed in cooled 90% ethanol/5% acetic acid for 20 min. Then the nuclei were stained with Hoechst 3342 (Sigma). Image acquisition and analysis were performed using a Cellomics ArrayScan VTI/HCS reader (Thermo Scientific).

Breast Cancer Cell Proliferation (MTT Assay). Cells were seeded at 1.5×10^4 cells/cm^2 in 24-well plates. After 24 h, the cells were grown for 72 h with inhibitors used over a 10^{-9} to 10 μM concentration range. Cell proliferation was assessed with the MTT assay. Briefly, the cells were incubated with 400 μL of MTT (0.5 mg/mL in culture medium) for 1 h at 37 °C. The medium was then aspirated. Formazan crystals were dissolved with 400 μL dimethyl sulfoxide for 5 min. The absorbance of each well was read at 570 nm in a Spectramax 190 spectrophotometer (Molecular Devices Corp., Sunnyvale, CA). The assay was performed in three wells per condition. Absorbance is expressed as a percentage of the control (vehicle).

Cell Cycle Analysis. Cells were grown in the presence of inhibitors for 24 h. Breast cancer cells were treated with the Coulter DNA-Prep reagents kit (Beckman Coulter, France) as previously described.[52] Flow cytometry analyses were performed using a Coulter Epics Elite ESP flow cytometer (Beckman Coulter). Cell cycle distribution was analyzed with the Multicycle-AV software (Phoenix Flow Systems, San Diego, CA).

Quantification of Apoptotic Cells. Cells were grown in the presence of inhibitors for 48 h. Apoptosis was assessed by flow cytometry with a method adapted to adherent cells, which is based on the selective thermal denaturation of apoptotic DNA and detection of denatured DNA with a monoclonal antibody against single-stranded DNA (anti-ssDNA Mab, F7−26, from AbCys, Paris, France). The cells were treated as previously described.[52] Data were analyzed with the Expo32 software (Beckman Coulter, France).

Western Blot Analysis. Cells were grown in the presence of inhibitors for 48 h. Cellular lysates (PBS/5% SDS lysis buffer containing protease inhibitors and phosphatase inhibitors) were subjected to SDS−polyacrylamide (10%) gel electrophoresis and transferred onto nitrocellulose membranes. Immunoblotting was done using rabbit monoclonal antibodies (Cell Signaling Technology, Ozyme, France) against Akt phosphorylated on Thr 308 (ref 4056) or Ser 473 (ref 4060) and total Akt (ref 4685) and against S6K1

phosphorylated on Thr 389 (ref 9234) and total S6K1 (ref 2708). Detection was performed with the enhanced chemiluminescence reagent (ECL Western blotting detection reagents, Interchim, France). Bands were quantitated using the Multi Gauge software (Fujifilm).

Statistical Analysis. Statistical analysis was performed using the GraphPad Prism software. Data are presented as the mean ± SD from at least three independent experiments, and differences are considered significant when $P < 0.05$ as determined by the nonparametric unpaired Student t test.

■ ASSOCIATED CONTENT

Ⓢ Supporting Information

Additional characterizations for compounds **2–13**, ^1H and ^{13}C NMR spectra for compounds **2–13**, and standard deviations for IC_{50} (Table S1). This material is available free of charge via the Internet at http://pubs.acs.org.

Accession Codes

Crystal structure PDB IDs for docking model construction used in this paper: 3HHM, 3IEB.

■ AUTHOR INFORMATION

Corresponding Author

*Phone: 33 238 494 853. Fax: 33 238 417 281. E-mail: sylvain.routier@univ-orleans.fr.

Notes

The authors declare no competing financial interest.

■ ACKNOWLEDGMENTS

■ ABBREVIATIONS USED

EtOAc, ethyl acetate; nM, nanomolar; μM, micromolar; μL, microliter; vs, versus; ATR, attenuated total reflection; mg, milligram; satd, saturated; IS, ion spray; RTKs, several receptor tyrosine kinases; GPCRs, G-protein-coupled receptors; PI3K, phosphoinositide 3-kinase; PIP2, phosphatidylinositol 4,5-diphosphate; PIP3, phosphatidylinositol 3,4,5-triphosphate; mTOR, mammalian target of rapamycin; IRS-1, insulin receptor substrate 1; SAR, structure–activity relationship; MW, microwave; Ac₂O, acetic anhydride; DMF, dimethylformamide; EtOH, ethanol; rflx, reflux; MOM, methyl methyl ether; DYRK, dual-specificity tyrosine-phosphorylation-regulated kinase; CK, cyclin kinase; GSK, glycogen synthase kinase; FDA, Food and Drug Administration

■ REFERENCES

(1) (a) Cantley, L. C. The phosphoinositide 3-kinase pathway. *Science* **2002**, *296*, 1655–1657. (b) Engelman, J. A.; Luo, J.; Cantley, L. C. The evolution of phosphatidylinositol 3-kinases as regulators of growth and metabolism. *Nat. Rev. Genet.* **2006**, *7*, 606–619.

(2) Meier, T. I.; Cook, J. A.; Thomas, J. E.; Radding, J. A.; Horn, C.; Lingaraj, T.; Smith, M. C. Cloning, expression, purification, and characterization of the human class Ia phosphoinositide 3-kinase isoforms. *Protein Expression Purif.* **2004**, *35*, 218–224.

(3) Ali, K.; Camps, M.; Pearce, W. P.; Ji, H.; Rückle, T.; Kuehn, N.; Pasquali, C.; Chabert, C.; Rommel, C.; Vanhaesebroeck, B. Isoform-specific functions of phosphoinositide 3-kinases: p110δ but not p110γ promotes optimal allergic responses in vivo. *J. Immunol.* **2008**, *180*, 2538–2544.

(4) Ali, K.; Bilancio, A.; Thomas, M.; Pearce, W.; Gilfillan, A. M.; Tkaczyk, C.; Kuehn, N.; Gray, A.; Giddings, J.; Peskett, E.; Fox, R.; Bruce, I.; Walker, C.; Sawyer, C.; Okkenhaug, K.; Finan, P.; Vanhaesebroeck, B. Essential role for the p110δ phosphoinositide 3-kinase in the allergic response. *Nature* **2004**, *431*, 1007–1011.

(5) Jackson, S. P.; Schoenwaelder, S. M.; Goncalves, I.; Nesbitt, W. S.; Yap, C. L.; Wright, C. E.; Kenche, V.; Anderson, K. E.; Dopheide, S. M.; Yuan, Y.; Sturgeon, S. A.; Prabaharan, H.; Thompson, P. E.; Smith, G. D.; Shepherd, P. R.; Daniele, N.; Kulkarni, S.; Abbott, B.; Saylik, D.; Jones, C.; Lu, L.; Giuliano, S.; Hughan, S. C.; Angus, J. A.; Robertson, A. D.; Salem, H. H. PI3-kinase p110β: a new target for antithrombotic therapy. *Nat. Med.* **2005**, *11*, 507–514.

(6) Hirsch, E.; Katanaev, V. L.; Garlanda, C.; Azzolino, O.; Pirola, L.; Silengo, L.; Sozzani, S.; Mantovani, A.; Altruda, F.; Wymann, M. P. Central role for G protein-coupled phosphoinositide 3-kinase γ in inflammation. *Science* **2000**, *287*, 1049–1053.

(7) Campbell, I. G.; Russell, S. E.; Choong, D. Y. H.; Montgomery, K. G.; Ciavarella, M. L.; Hooi, C. S. F.; Cristiano, B. E.; Pearson, R. B.; Phillips, W. A. Mutation of the PIK3CA gene in ovarian and breast cancer. *Cancer Res.* **2004**, *64*, 7678–7681.

(8) Kang, S.; Bader, A. G.; Vogt, P. K. Phosphatidylinositol 3-kinase mutations identified in human cancer are oncogenic. *Proc. Natl. Acad. Sci. U.S.A.* **2005**, *102*, 802–807.

(9) Samuels, Y.; Wang, Z.; Bardelli, A.; Silliman, N.; Ptak, J.; Szabo, S.; Yan, H.; Gazdar, A.; Powell, S. M.; Riggins, G. J.; Willson, J. K. V.; Markowitz, S.; Kinzler, K. W.; Vogelstein, B.; Velculescu, V. E. High frequency of mutations of the PIK3CA gene in human cancers. *Science* **2004**, *304*, 554.

(10) Yuan, T. L.; Cantley, L. C. PI3K pathway alterations in cancer: variations on a theme. *Oncogene* **2008**, *27*, 5497–5510.

(11) Manning, B. D. Balancing Akt with S6K: implications for both metabolic diseases and tumorigenesis. *J. Cell Biol.* **2004**, *167*, 399–403.

(12) Liu, P.; Cheng, H.; Roberts, T. M.; Zhao, J. J. Targeting the phosphoinositide 3-kinase pathway in cancer. *Nat. Rev. Drug Discovery* **2009**, *8*, 627–644.

(13) Jiang, B.-H.; Liu, L.-Z. Role of mTOR in anticancer drug resistance: perspectives for improved drug treatment. *Drug Resist. Updates* **2008**, *11*, 63–76.

(14) (a) Chalhoub, N.; Baker, S. J. PTEN and the PI3-kinase pathway in cancer. *Annu. Rev. Pathol.* **2009**, *4*, 127–150. (b) O'Reilly, K. E.; Rojo, F.; She, Q.-B.; Solit, D.; Mills, G. B.; Smith, D.; Lane, H.; Hofmann, F.; Hicklin, D. J.; Ludwig, D. L.; Baselga, J.; Rosen, N. mTOR inhibition induces upstream receptor tyrosine kinase signaling and activates Akt. *Cancer Res.* **2006**, *66*, 1500–1508.

(15) Peng, T.; Golub, T. R.; Sabatini, D. M. The immunosuppressant rapamycin mimics a starvation-like signal distinct from amino acid and glucose deprivation. *Mol. Cell. Biol.* **2002**, *22*, 5575–5584.

(16) Shaw, R. J.; Cantley, L. C. Ras, PI3K and mTOR signalling controls tumour cell growth. *Nature* **2006**, *441*, 424–430.

(17) Cleary, J. M.; Shapiro, G. I. Development of phosphoinositide-3 kinase pathway inhibitors for advanced cancer. *Curr. Oncol. Rep.* **2010**, *12*, 87–94.

(18) Garcia-Echeverria, C.; Sellers, W. R. Drug discovery approaches targeting the PI3K/Akt pathway in cancer. *Oncogene* **2008**, *27*, 5511–5526.

(19) (a) Mahadevan, D.; Chiorean, E. G.; Harris, W. B.; Von Hoff, D. D.; Stejskal-Barnett, A.; Qi, W.; Anthony, S. P.; Younger, A. E.; Rensvold, D. M.; Cordova, F.; Shelton, C. F.; Becker, M. D.; Garlich, J. R.; Durden, D. L.; Ramanathan, R. K. Phase I pharmacokinetic and pharmacodynamic study of the pan-PI3K/mTORC vascular targeted pro-drug SF1126 in patients with advanced solid tumours and B-cell malignancies. *Eur. J. Cancer* **2012**, *48*, 3319–3327. (b) Chang, K.-Y.;

Tsai, S.-Y.; Wu, C.-M.; Yen, C.-J.; Chuang, B.-F.; Chang, J.-Y. Novel phosphoinositide 3-kinase/mTOR dual inhibitor, NVP-BGT226, displays potent growth-inhibitory activity against human head and neck cancer cells in vitro and in vivo. *Clin. Cancer Res.* **2011**, *17*, 7116−7126. (c) Cleary, J. M.; Shapiro, G. I. Development of phosphoinositide-3 kinase pathway inhibitors for advanced cancer. *Curr. Oncol. Rep.* **2010**, *12*, 87−94. (d) Ihle, N. T.; Powis, G. Take your PIK: phosphatidylinositol 3-kinase inhibitors race through the clinic and toward cancer therapy. *Mol. Cancer Ther.* **2009**, *8*, 1−9. (e) Marone, R.; Cmiljanovic, V.; Giese, B.; Wymann, M. P. Targeting phosphoinositide 3-kinase: moving towards therapy. *Biochim. Biophys. Acta* **2008**, *1784*, 159−185. (f) Yap, T. A.; Garrett, M. D.; Walton, M. I.; Raynaud, F.; De Bono, J. S.; Workman, P. Targeting the PI3K-AKT-mTOR pathway: progress, pitfalls, and promises. *Curr. Opin. Pharmacol.* **2008**, *8*, 393−412. (g) Eichhorn, P. J. A.; Gili, M.; Scaltriti, M.; Serra, V.; Guzman, M.; Nijkamp, W.; Beijersbergen, R. L.; Valero, V.; Seoane, J.; Bernards, R.; Baselga, J. Phosphatidylinositol 3-kinase hyperactivation results in lapatinib resistance that is reversed by the mTOR/phosphatidylinositol 3-kinase inhibitor NVP-BEZ235. *Cancer Res.* **2008**, *68*, 9221−9230. (h) Maira, S.-M.; Stauffer, F.; Brueggen, J.; Furet, P.; Schnell, C.; Fritsch, C.; Brachmann, S.; Chène, P.; Pover, A. D.; Schoemaker, K.; Fabbro, D.; Gabriel, D.; Simonen, M.; Murphy, L.; Finan, P.; Sellers, W.; García-Echeverría, C. Identification and characterization of NVP-BEZ235, a new orally available dual phosphatidylinositol 3-kinase/mammalian target of rapamycin inhibitor with potent in vivo antitumor activity. *Mol. Cancer Ther.* **2008**, *7*, 1851−1863. (i) Howes, A. L.; Chiang, G. G.; Lang, E. S.; Ho, C. B.; Powis, G.; Vuori, K.; Abraham, R. T. The phosphatidylinositol 3-kinase inhibitor, PX-866, is a potent inhibitor of cancer cell motility and growth in three-dimensional cultures. *Mol. Cancer Ther.* **2007**, *6*, 2505−2514. (j) Phase I Trial of Oral PX-866. http://www.clinicaltrials.gov/ct2/show/NCT00726583?term=PX866&rank=5 (accessed January 2014).

(20) (a) Liu, Q.; Thoreen, C.; Wang, J.; Sabatini, D.; Gray, N. S. mTOR mediated anti-cancer drug discovery. *Drug Discovery Today: Ther. Strategies* **2009**, *6*, 47−55. (b) Apsel, B.; Blair, J. A.; Gonzalez, B.; Nazif, T. M.; Feldman, M. E.; Aizenstein, B.; Hoffman, R.; Williams, R. L.; Shokat, K. M.; Knight, Z. A. Targeted polypharmacology: discovery of dual inhibitors of tyrosine and phosphoinositide kinases. *Nat. Chem. Biol.* **2008**, *4*, 691−699.

(21) (a) Liu, K. K. C.; Huang, X.; Bagrodia, S.; Chen, J. H.; Greasley, S.; Cheng, H.; Sun, S.; Knighton, D.; Rodgers, C.; Rafidi, K.; Zou, A.; Xiao, J.; Yan, S. Quinazolines with intra-molecular hydrogen bonding scaffold (iMHBS) as PI3K/mTOR dual inhibitors. *Bioorg. Med. Chem. Lett.* **2011**, *21*, 1270−1274. (b) Liu, K. K.-C.; Bagrodia, S.; Bailey, S.; Cheng, H.; Chen, H.; Gao, L.; Greasley, S.; Hoffman, J. E.; Hu, Q.; Johnson, T. O.; Knighton, D.; Liu, Z.; Marx, M. A.; Nambu, M. D.; Ninkovic, S.; Pascual, B.; Rafidi, K.; Rodgers, C. M.-L.; Smith, G. L.; Sun, S.; Wang, H.; Yang, A.; Yuan, J.; Zou, A. 4-Methylpteridinones as orally active and selective PI3K/mTOR dual inhibitors. *Bioorg. Med. Chem. Lett.* **2010**, *20*, 6096−6099.

(22) (a) Cheng, H.; Bagrodia, S.; Bailey, S.; Edwards, M.; Hoffman, J.; Hu, Q.; Kania, R.; Knighton, D. R.; Marx, M. A.; Ninkovic, S.; Sun, S.; Zhang, E. Discovery of the highly potent PI3K/mTOR dual inhibitor PF-04691502 through structure based drug design. *MedChemComm* **2010**, *1*, 139. (b) Knight, S. D.; Adams, N. D.; Burgess, J. L.; Chaudhari, A. M.; Darcy, M. G.; Donatelli, C. A.; Luengo, J. I.; Newlander, K. A.; Parrish, C. A.; Ridgers, L. H.; Sarpong, M. A.; Schmidt, S. J.; Van Aller, G. S.; Carson, J. D.; Diamond, M. A.; Elkins, P. A.; Gardiner, C. M.; Garver, E.; Gilbert, S. A.; Gontarek, R. R.; Jackson, J. R.; Kershner, K. L.; Luo, L.; Raha, K.; Sherk, C. S.; Sung, C.-M.; Sutton, D.; Tummino, P. J.; Wegrzyn, R. J.; Auger, K. R.; Dhanak, D. Discovery of GSK2126458, a highly potent inhibitor of PI3K and the mammalian target of rapamycin. *ACS Med. Chem. Lett.* **2010**, *1*, 39−43. (c) Wen, P. Y.; Omuro, A. M.; Batchelor, T. T.; Lai, A.; Mellinghoff, I. K.; Nghiemphu, L.; Norden, A.; Gendreau, S. B.; Laird, A. D.; Nguyen, L.; Cloughesy, T. Abstract B265: a phase 1 safety and pharmacokinetic study of XL765 (SAR245409), a novel PI3K/TORC1/TORC2 inhibitor, in combination with temozolomide

(TMZ) in patients (pts) with malignant glioma. *Mol. Cancer Ther.* **2009**, *8*, B265−B265.

(23) (a) Tikad, A.; Routier, S.; Akssira, M.; Léger, J.-M.; Jarry, C.; Guillaumet, G. Efficient synthesis of 2-substituted pyrido[3,2-*d*]pyrimidines involving S$_N$Ar and palladium-catalyzed cross-coupling reactions. *Synthesis* **2009**, 2379−2284. (b) Tikad, A.; Routier, S.; Akssira, M.; Guillaumet, G. Efficient one-pot synthesis of 2,4-di(het)aryl and 2,4-diamino pyrido[3,2-*d*]pyrimidines involving regioselective S$_N$Ar and palladium-catalyzed reactions. *Org. Biomol. Chem.* **2009**, *7*, 5113−5118. (c) Tikad, A.; Routier, S.; Akssira, M.; Leger, J.-M.; Jarry, C.; Guillaumet, G. New efficient route to dissymmetric 2,4-di(het)aryl-pyrido[3,2-*d*]pyrimidines via regioselective cross-coupling reactions. *Org. Lett.* **2007**, *9*, 4673−4676. (d) Tikad, A.; Routier, S.; Akssira, M.; Leger, J.-M.; Jarry, C.; Guillaumet, G. Efficient access to novel mono- and disubstituted pyrido[3,2-*d*]pyrimidines. *Synlett* **2006**, 1938−1942.

(24) (a) Hayakawa, M.; Kaizawa, H.; Moritomo, H.; Koizumi, T.; Ohishi, T.; Okada, M.; Ohta, M.; Tsukamoto, S.; Parker, P.; Workman, P.; Waterfield, M. Synthesis and biological evaluation of 4-morpholino-2-phenylquinazolines and related derivatives as novel PI3 kinase p110α inhibitors. *Bioorg. Med. Chem.* **2006**, *14*, 6847−6858. (b) Hayakawa, M.; Kaizawa, H.; Moritomo, H.; Kawaguchi, K.; Koizumi, T.; Yamano, M.; Matsuda, K.; Okada, M.; Ohta, M. Preparation of condensed heteroaryl derivatives as phosphatidylinositol 3-kinase inhibitors and anticancer agents. PCT Int. Appl. WO 2001083456 A1 20011108, 2001. (c) Sutherlin, D. P.; Baker, S.; Bisconte, A.; Blaney, P. M.; Brown, A.; Chan, B. K.; Chantry, D.; Castanedo, G.; DePledge, P.; Goldsmith, P.; Goldstein, D. M.; Hancox, T.; Kaur, J.; Knowles, D.; Kondru, R.; Lesnick, J.; Lucas, M. C.; Lewis, C.; Murray, J.; Nadin, A. J.; Nonomiya, J.; Pang, J.; Pegg, N.; Price, S.; Reif, K.; Safina, B. S.; Salphati, L.; Staben, S.; Seward, E. M.; Shuttleworth, S.; Sohal, S.; Sweeney, Z. K.; Ultsch, M.; Waszkowycz, B.; Wei, B. Potent and selective inhibitors of PI3Kδ: obtaining isoform selectivity from the affinity pocket and tryptophan shelf. *Bioorg. Med. Chem. Lett.* **2012**, *22*, 4296−4302.

(25) Vlahos, C. J.; Matter, W. F.; Hui, K. Y.; Brown, R. F. A specific inhibitor of phosphatidylinositol 3-kinase, 2-(4-morpholinyl)-8-phenyl-4H-1-benzopyran-4-one (LY294002). *J. Biol. Chem.* **1994**, *269*, 5241−5248.

(26) Pomel, V.; Gaillard, P.; Desforges, G.; Quattropani, A.; Montagne, C. Preparation of 4-morpholino-pyrido[3,2-*d*]pyrimidine compounds as PI3K inhibitors for therapeutic applications. PCT Int. Appl. WO 2010037765 A2 20100408, 2010.

(27) Castanedo, G.; Chan, B.; Lucas, M.; Safina, B.; Sutherlin, D.; Sweeney, Z. Preparation of pyrido[3,2-*d*]pyrimidine as PI3kδ inhibitors. PCT Int. Appl. WO 2011101429 A1 20110825, 2011.

(28) Folkes, A. J.; Ahmadi, K.; Alderton, W. K.; Alix, S.; Baker, S. J.; Box, G.; Chuckowree, I. S.; Clarke, P. A.; Depledge, P.; Eccles, S. A.; Friedman, L. S.; Hayes, A.; Hancox, T. C.; Kugendradas, A.; Lensun, L.; Moore, P.; Olivero, A. G.; Pang, J.; Patel, S.; Pergl-Wilson, G. H.; Raynaud, F. I.; Robson, A.; Saghir, N.; Salphati, L.; Sohal, S.; Ultsch, M. H.; Valenti, M.; Wallweber, H. J. A.; Wan, N. C.; Wiesmann, C.; Workman, P.; Zhyvoloup, A.; Zvelebil, M. J.; Shuttleworth, S. J. The identification of 2-(1*H*-indazol-4-yl)-6-(4-methanesulfonyl-piperazin-1-ylmethyl)-4-morpholin-4-yl-thieno[3,2-*d*]pyrimidine (GDC-0941) as a potent, selective, orally bioavailable inhibitor of class I PI3 kinase for the treatment of cancer. *J. Med. Chem.* **2008**, *51*, 5522−5532.

(29) Sutherlin, D. P.; Sampath, D.; Berry, M.; Castanedo, G.; Chang, Z.; Chuckowree, I.; Dotson, J.; Folkes, A.; Friedman, L.; Goldsmith, R.; Heffron, T.; Lee, L.; Lesnick, J.; Lewis, C.; Mathieu, S.; Nonomiya, J.; Olivero, A.; Pang, J.; Prior, W. W.; Salphati, L.; Sideris, S.; Tian, Q.; Tsui, V.; Wan, N. C.; Wang, S.; Wiesmann, C.; Wong, S.; Zhu, B.-Y. Discovery of (thienopyrimidin-2-yl)aminopyrimidines as potent, selective, and orally available pan-PI3-kinase and dual pan-PI3-kinase/mTOR inhibitors for the treatment of cancer. *J. Med. Chem.* **2010**, *53*, 1086−1097.

(30) (a) Lavecchia, G.; Berteina-Raboin, S.; Guillaumet, G. Selective bifunctionalization of pyrido[2,3-*d*]pyrimidines in positions 2 and 4 by S$_N$Ar and palladium-catalyzed coupling reactions. *Tetrahedron Lett.*

2005, 46, 5851−5855. (b) Riadi, Y.; Massip, S.; Leger, J. M.; Jarry, C.; Lazar, S.; Guillaumet, G. Convenient synthesis of 2,4-disubstituted pyrido[2,3-d]pyrimidines via regioselective palladium-catalyzed reactions. Tetrahedron 2012, 68, 5018−5024.

(31) Neagoie, C.; Vedrenne, E.; Buron, F.; Mérour, J.-Y.; Rosca, S.; Bourg, S.; Lozach, O.; Meijer, L.; Baldeyrou, B.; Lansiaux, A.; Routier, S. Synthesis of chromeno[3,4-b]indoles as lamellarin D analogues: a novel DYRK1A inhibitor class. Eur. J. Med. Chem. 2012, 49, 379−396.

(32) (a) Verheijen, J. C.; Richard, D. J.; Curran, K.; Kaplan, J.; Lefever, M.; Nowak, P.; Malwitz, D. J.; Brooijmans, N.; Toral-Barza, L.; Zhang, W.-G.; Lucas, J.; Hollander, I.; Ayral-Kaloustian, S.; Mansour, T. S.; Yu, K.; Zask, A. Discovery of 4-morpholino-6-aryl-1H-pyrazolo[3,4-d]pyrimidines as highly potent and selective ATP-competitive inhibitors of the mammalian target of rapamycin (mTOR): optimization of the 6-aryl substituent. J. Med. Chem. 2009, 52, 8010−8024. (b) Smith, R.; Thompson, S.; Hosahalli, S.; Bejugam, M.; Nanduri, S.; Panigrahi, S.; Mahalingam, N. Preparation of morpholinylheteroaryl-quinazolinylphenylcarbonylphenylurea derivatives and analogs for use as dual PI3K/mTOR inhibitors. PCT Int. Appl. WO 2012058671 A1 20120503, 2012.

(33) Biological Macromolecular Resource. http://www.rcsb.org/pdb/home/home.do (accessed January 2014).

(34) Huang, C.-H.; Mandelker, D.; Schmidt-Kittler, O.; Samuels, Y.; Velculescu, V. E.; Kinzler, K. W.; Vogelstein, B.; Gabelli, S. B.; Amzel, L. M. The structure of a human p110α/p85α complex elucidates the effects of oncogenic PI3Kα mutations. Science 2007, 318, 1744−1748.

(35) Mandelker, D.; Gabelli, S. B.; Schmidt-Kittler, O.; Zhu, J.; Cheong, I.; Huang, C.-H.; Kinzler, K. W.; Vogelstein, B.; Amzel, L. M. A frequent kinase domain mutation that changes the interaction between PI3Kα and the membrane. Proc. Natl. Acad. Sci. U.S.A. 2009, 106, 16996−17001.

(36) Knight, Z. A.; Chiang, G. G.; Alaimo, P. J.; Kenski, D. M.; Ho, C. B.; Coan, K.; Abraham, R. T.; Shokat, K. M. Isoform-specific phosphoinositide 3-kinase inhibitors from an arylmorpholine scaffold. Bioorg. Med. Chem. 2004, 12, 4749−4759.

(37) Zask, A.; Verheijen, J. C.; Curran, K.; Kaplan, J.; Richard, D. J.; Nowak, P.; Malwitz, D. J.; Brooijmans, N.; Bard, J.; Svenson, K.; Lucas, J.; Toral-Barza, L.; Zhang, W.-G.; Hollander, I.; Gibbons, J. J.; Abraham, R. T.; Ayral-Kaloustian, S.; Mansour, T. S.; Yu, K. ATP-competitive inhibitors of the mammalian target of rapamycin: design and synthesis of highly potent and selective pyrazolopyrimidines. J. Med. Chem. 2009, 52, 5013−5016.

(38) Friesner, R. A.; Banks, J. L.; Murphy, R. B.; Halgren, T. A.; Klicic, J. J.; Mainz, D. T.; Repasky, M. P.; Knoll, E. H.; Shelley, M.; Perry, J. K.; Shaw, D. E.; Francis, P.; Shenkin, P. S. Glide: a new approach for rapid, accurate docking and scoring. 1. Method and assessment of docking accuracy. J. Med. Chem. 2004, 47, 1739−1749.

(39) Nakabayashi, H.; Taketa, K.; Miyano, K.; Yamane, T.; Sato, J. Growth of human hepatoma cells lines with differentiated functions in chemically defined medium. Cancer Res. 1982, 42, 3858−3863.

(40) Nakanishi, K.; Fujimoto, J.; Ueki, T.; Kishimoto, K.; Hashimoto-Tamaoki, T.; Furuyama, J.; Itoh, T.; Sasaki, Y.; Okamoto, E. Hepatocyte growth factor promotes migration of human hepatocellular carcinoma via phosphatidylinositol 3-kinase. Clin. Exp. Metastasis 1999, 17, 507−514.

(41) Gedaly, R.; Angulo, P.; Hundley, J.; Daily, M. F.; Chen, C.; Koch, A.; Evers, B. M. PI-103 and sorafenib inhibit hepatocellular carcinoma cell proliferation by blocking Ras/Raf/MAPK and PI3K/AKT/mTOR pathways. Anticancer Res. 2010, 30, 4951−4958.

(42) Ivison, S. M.; Khan, M. A. S.; Graham, N. R.; Shobab, L. A.; Yao, Y.; Kifayet, A.; Sly, L. M.; Steiner, T. S. The p110α and p110β isoforms of class I phosphatidylinositol 3-kinase are involved in Toll-like receptor 5 signaling in epithelial cells. Mediators Inflammation 2010, 1−12.

(43) Langlois, M.-J.; Bergeron, S.; Bernatchez, G.; Boudreau, F.; Saucier, C.; Perreault, N.; Carrier, J. C.; Rivard, N. The PTEN phosphatase controls intestinal epithelial cell polarity and barrier function: role in colorectal cancer progression. PLoS One 2010, 5, e15742.

(44) Mordant, P.; Loriot, Y.; Leteur, C.; Calderaro, J.; Bourhis, J.; Wislez, M.; Soria, J.-C.; Deutsch, E. Dependence on phosphoinositide 3-kinase and RAS-RAF pathways drive the activity of RAF265, a novel RAF/VEGFR2 inhibitor, and RAD001 (everolimus) in combination. Mol. Cancer Ther. 2010, 9, 358−368.

(45) Bénistant, C.; Chapuis, H.; Roche, S. A specific function for phosphatidylinositol 3-kinase α (p85α-p110α) in cell survival and for phosphatidylinositol 3-kinase β (p85α-p110β) in de novo DNA synthesis of human colon carcinoma cells. Oncogene 2000, 19, 5083−5090.

(46) Calay, D.; Vind-Kezunovic, D.; Frankart, A.; Lambert, S.; Poumay, Y.; Gniadecki, R. Inhibition of Akt signaling by exclusion from lipid rafts in normal and transformed epidermal keratinocytes. J. Invest. Dermatol. 2010, 130, 1136−1145.

(47) Hollestelle, A.; Elstrodt, F.; Nagel, J. H. A.; Kallemeijn, W. W.; Schutte, M. Phosphatidylinositol-3-OH kinase or RAS pathway mutations in human breast cancer cell lines. Mol. Cancer Res. 2007, 5, 195−201.

(48) Clark, A. S.; West, K.; Streicher, S.; Dennis, P. A. Constitutive and inducible Akt activity promotes resistance to chemotherapy, trastuzumab, or tamoxifen in breast cancer cells. Mol. Cancer Ther. 2002, 1, 707−717.

(49) Maestro, version 9.1, Glide, version 5.6, MacroModel, version 9.8, Schrödinger, LLC, New York, 2010.

(50) Marvin 5.3.6, ChemAxon, 2010. http://www.chemaxon.com (accessed January 2014).

(51) (a) Sadowski, J.; Gasteiger, J. From atoms and bonds to three-dimensional atomic coordinates: automatic model builders. Chem. Rev. 1993, 93, 2567−2581. (b) CORINA—Fast Generation of High-Quality 3D Molecular Models. http://www.molecular-networks.com/products/corina (accessed January 2014).

(52) Barascu, A.; Besson, P.; Le Floch, O.; Bougnoux, P.; Jourdan, M.-L. CDK1-cyclin B1 mediates the inhibition of proliferation induced by omega-3 fatty acids in MDA-MB-231 breast cancer cells. Int. J. Biochem. Cell Biol. 2006, 38, 196−208.